

A Transmembrane Guanylyl Cyclase (DAF-11) and Hsp90 (DAF-21) Regulate a Common Set of Chemosensory Behaviors in *Caenorhabditis elegans*

Deborah A. Birnby,^{1,2} Elizabeth Malone Link,^{1,3} Jennifer J. Vowels,² Hong Tian, Patrick L. Colacurcio and James H. Thomas

Department of Genetics, University of Washington, Seattle, Washington 98195-7360

Manuscript received November 4, 1999
Accepted for publication January 10, 2000

ABSTRACT

Caenorhabditis elegans *daf-11* and *daf-21* mutants share defects in specific chemosensory responses mediated by several classes of sensory neurons, indicating that these two genes have closely related functions in an assortment of chemosensory pathways. We report that *daf-11* encodes one of a large family of *C. elegans* transmembrane guanylyl cyclases (TM-GCs). The cyclic GMP analogue 8-bromo-cGMP rescues a sensory defect in both *daf-11* and *daf-21* mutants, supporting a role for DAF-11 guanylyl cyclase activity in this process and further suggesting that *daf-21* acts at a similar step. *daf-11::gfp* fusions are expressed in five identified pairs of chemosensory neurons in a pattern consistent with most *daf-11* mutant phenotypes. We also show that *daf-21* encodes the heat-shock protein 90 (Hsp90), a chaperone with numerous specific protein targets. We show that the viable chemosensory-deficient *daf-21* mutation is an unusual allele resulting from a single amino acid substitution and that the *daf-21* null phenotype is early larval lethality. These results demonstrate that cGMP is a prominent second messenger in *C. elegans* chemosensory transduction and suggest a previously unknown role for Hsp90 in regulating cGMP levels.

LIKE all free-living organisms, *Caenorhabditis elegans* responds to a variety of environmental stimuli. The presence of food affects locomotion, egg laying, and defecation (B. Sawin, C. Trent and H. R. Horvitz, personal communication; Liu and Thomas 1994). Specific volatile and nonvolatile chemicals attract or repel *C. elegans* in chemotaxis assays (Ward 1973; Dusenbery 1974; Bargmann *et al.* 1993), and a constitutively secreted pheromone regulates development (Golden and Riddle 1982, 1984a). *daf-11* and *daf-21* mutants have similar defects in several of these responses (reviewed in Riddle and Albert 1997), suggesting that the *daf-11* and *daf-21* gene products (DAF-11 and DAF-21) act at the same step to regulate chemosensory transduction in several types of sensory neurons.

In *C. elegans*, bilaterally symmetric pairs of ciliated sensory neurons in the head amphid sensilla mediate many chemosensory behaviors. For example, *C. elegans* is attracted to a variety of nonvolatile chemicals, including Cl⁻, cAMP, and biotin, which are sensed primarily by the ASE neurons (Bargmann and Horvitz 1991b). Response to these attractants is defective in both *daf-11* and *daf-21* mutants (Vowels and Thomas 1994). *C. ele-*

gans is also attracted to several volatile odorants, and different chemical classes are detected by the AWA, AWB, and AWC neurons (Bargmann *et al.* 1993). *daf-11* and *daf-21* mutants do not respond to isoamyl alcohol and benzaldehyde, which are sensed by the AWC neurons, but respond normally to odorants sensed by the AWA neurons (Vowels and Thomas 1994). These mutant phenotypes suggest that both *daf-11* and *daf-21* mutants have functional deficits in two classes of sensory neurons, ASE and AWC.

The external environment also regulates formation of the *C. elegans* dauer larva, an alternative third-stage larva specialized for survival under harsh conditions (Cassada and Russell 1975). A constitutively secreted pheromone is the main inducer of dauer formation (Golden and Riddle 1982, 1984a). Temperature and food modulate the effect of this pheromone, with high temperature and low food levels favoring dauer formation (Golden and Riddle 1984a,b). *daf-11* and *daf-21* mutants are Daf-c (*dauer formation constitutive*), forming dauers even in the absence of inducing conditions (Riddle *et al.* 1981; Thomas *et al.* 1993). In addition to *daf-11* and *daf-21*, several other genes regulate dauer formation, and most of these genes have been ordered into a genetic pathway by analysis of double mutants (reviewed in Riddle and Albert 1997). The Daf-c genes *daf-1*, *-4*, *-7*, *-8*, and *-14* are thought to act in parallel to *daf-11* and *-21* (Thomas *et al.* 1993) and encode components of a TGF- β -like signaling pathway (Georgi *et al.* 1990; Estevez *et al.* 1993; Ren *et al.* 1996; Inoue and Thomas 2000; A. Estevez and D. L. Riddle, personal

Corresponding author: James H. Thomas, Department of Genetics, Box 357360, University of Washington, Seattle, WA 98195-7360.
E-mail: jht@genetics.washington.edu

¹ These authors contributed equally to this work.

² Present address: QIAGEN Inc., 28159 Avenue Stanford, Valencia, CA 91355.

³ Present address: Cambria Biosciences, LLC, 2 Preston Ct., Medford, MA 01730.

communication). The Daf-c genes *daf-2* and *age-1* are thought to act in parallel to or downstream of *daf-11* and *-21* (Thomas *et al.* 1993; Gottlieb and Ruvkun 1994) and encode components of an insulin-like signaling pathway (Kimura *et al.* 1994; Morris *et al.* 1996). It is notable that analyses of pleiotropic mutant phenotypes and double mutant interactions have all identified shared properties of *daf-11* and *daf-21* mutants that are distinct from other Daf-c mutants (reviewed in Riddle and Albert 1997).

Regulation of dauer formation is also mediated by particular classes of amphid sensory neurons, and the functions of these neurons have been determined by killing specified cells with a laser microbeam. When the ADF and ASI neurons are killed together, wild-type larvae form dauers constitutively (Bargmann and Horvitz 1991a; Schackwitz *et al.* 1996), indicating that these neurons normally repress dauer formation in the absence of inducing conditions. Varied evidence suggests that ADF and ASI mediate the function of the TGF- β -like signaling branch of the dauer pathway (Bargmann and Horvitz 1991a; Thomas *et al.* 1993; Schackwitz *et al.* 1996). In contrast, the ASJ neurons promote dauer formation, since killing these cells suppresses dauer formation in response to pheromone (Schackwitz *et al.* 1996). Killing the ASJ neurons also suppresses the constitutive dauer formation of *daf-11* and *daf-21* mutants, suggesting that the Daf-c phenotype in these mutants results from activation of ASJ (Schackwitz *et al.* 1996). Other Daf-c genes that function in the TGF- β -like signaling pathway or the insulin-like signaling pathway are distinct in that their Daf-c phenotype does not depend on the ASJ neurons. The ASJ neurons are also required for recovery from the dauer state (Bargmann and Horvitz 1991a) and *daf-21* and most *daf-11* dauers recover poorly (Vowels and Thomas 1994). Mutations that disrupt the amphid sensory cilia have been used in epistasis experiments to demonstrate that the Daf-c phenotype of *daf-11* and *daf-21* mutants requires intact ciliated sensory endings, suggesting that DAF-11 and DAF-21 function in the sensory endings to mediate an early step in chemosensory signal transduction (Vowels and Thomas 1992).

The various shared properties of *daf-11* and *daf-21* mutants indicate that these genes have closely related functions in several types of sensory neurons. Here we present molecular analyses of these two genes. We show that DAF-11 is homologous to transmembrane guanylyl cyclases (TM-GCs), which catalyze the formation of cyclic GMP (cGMP) from GTP. cGMP is a widely used second messenger that regulates kinases, other nucleotide cyclases, cyclic nucleotide phosphodiesterases, and cGMP-gated ion channels (reviewed in Goy 1991). We show that DAF-11 is one of a large family of TM-GCs predicted by the *C. elegans* Genome Sequencing Consortium, suggesting that cGMP is a common second messenger in *C. elegans*. Expression of a *daf-11::gfp* reporter

fusion is consistent with the known roles of DAF-11 in ASE, AWC, and ASJ. We demonstrate that a cGMP analogue rescues the Daf-c phenotypes of *daf-11* and *daf-21* mutants, indicating that in both cases the mutant phenotype results from reduced levels of cGMP. We also show that *daf-21* encodes heat-shock protein 90 (Hsp90), a chaperone protein that stabilizes many diverse protein targets. Our analysis indicates that the Daf-c *daf-21* mutation is an unusual allele and that a null mutation is lethal. We suggest a model in which Hsp90 is required to stabilize the DAF-11/TM-GC or another signal transduction component that regulates cGMP levels.

MATERIALS AND METHODS

Culture, strains, and genetics: *C. elegans* strain maintenance and genetic nomenclature were as described (Brenner 1974; Horvitz *et al.* 1979). The following strains were used: N2 (wild type), BW1435 *dpy-17(e164) ncl-1(e1865) unc-36(e251); him-8(e1490); her-1(y101hv1) unc-42(e270); ctDp11*, CB1364 *daf-4(e1364)*, CB1370 *daf-2(e1370)*, CB1372 *daf-7(e1372)*, DR20 *daf-12(m20)*, DR40 *daf-1(m40)*, DR77 *daf-14(m77)*, DR87 *daf-11(m87)*, JT191 *daf-28(sa191)*, JT195 *daf-11(sa195)*, JT5436 *daf-8(e1393)*, JT5850 *dpy-11(e224) daf-21(p673)*, JT5996 *sqt-3(sc63) daf-21(p673) unc-76(e911)*, JT6130 *daf-21(p673)*, JT6412 *daf-11(m84); daf-12(m20)*, JT6561 *daf-11(sa195); daf-12(m20)*, JT6672 *lon-3(e2175) daf-21(p673)*, JT6857 *dpy-17(e164) ncl-1(e1865) unc-36(e251); daf-21(p673); ctDp11*, JT6901 *dpy-17(e164) ncl-1(e1865) unc-36(e251); daf-11(sa195); ctDp11*, JT6917 *daf-4(e1364)*, JT6918 *daf-7(e1372)*, JT6919 *daf-14(m77)*, JT7672 *tax-4(ks11)*, JT7673 *tax-4(ks28)*, JT7674 *tax-4(p678)*, JT8708 *lon-3(e2175) daf-21(p673); saEx192* [pEM1; pRF4], JT8710 *lon-3(e2175) daf-21(p673) V; saEx193* [pEM1; pRF4], JT7839 *tax-4(ks11)*, JT7840 *tax-4(ks28)*, JT7841 *tax-4(p678)*, JT8712 *lon-3(e2175) daf-21(p673); saEx194* [pEM12; pRF4], JT8776 *lin-15(n765); saEx207*, JT8903 *lin-15(n765); saEx237*, JT8904 *lin-15(n765); saEx238*, JT9386 *daf11(sa195ts); saEx289*, KK 627 *itDf2/nT1 n754*, LL1008 *daf-21(nr2081)/nT1 n754*, and MT5813 *nDf42/nT1 n754*.

To map *daf-21(p673)* genetically, we crossed *him-5* males to *sqt-3 daf-21 unc-76/+ + +* hermaphrodites, picked non-Sqt non-Unc hermaphrodite cross-progeny, and then picked Sqt non-Unc and Unc non-Sqt recombinants in the next generation. The identification of recombinants was not biased by the *daf-21* genotype due to maternal rescue of the *daf-21* phenotype. We isolated strains homozygous for each recombinant chromosome and then scored the Him and Daf-c phenotypes. Of 23 Sqt non-Uncs, 15 were Him non-Daf, 6 were non-Him non-Daf, and 2 were Daf non-Him. Of 39 Unc non-Sqts, 25 were Daf non-Him, 9 were Daf Him, and 5 were Him non-Daf. These results are summarized in Figure 5A, and they indicate that *daf-21* is roughly two-thirds of the way between *him-5* and *unc-76*.

To test the nature of the *daf-21(p673)* mutation, we used deficiencies that delete the *daf-21* gene. Wild-type males were crossed to heterozygous hermaphrodites carrying chromosome V deficiencies balanced by the *nT1 n754* translocation. The dominant Unc phenotype of *n754* was used to infer the genotype of the progeny. Non-Unc males (*Df/+*) were crossed to *dpy-11 daf-21(p673)* hermaphrodites and the progeny were raised and scored at 20° or 25°. Individuals were picked and *daf-21(p673)/Df* strains were identified based on the segregation of dead eggs. Dpy progeny were assumed to be *daf-21(p673)* homozygotes, since *dpy-11* is linked to *daf-21*. We

tested three deficiencies that delete the *daf-21* region: *nDf42*, *itDf2*, and *yDf8*. All gave similar results.

The *daf-21(nr2081)* deletion was constructed *in trans* to the *nT1 n754* balancer translocation for strain maintenance. Wild-type males were crossed to *daf-21(nr2081)/+* heterozygotes and male progeny were crossed to *nDf42/nT1 n754* hermaphrodites. Unc progeny were picked, allowed to have progeny, and screened by PCR for *daf-21(nr2081)*. This procedure also served to outcross *daf-21(nr2081)* twice. We constructed *daf-21(p673)/daf-21(nr2081)* heterozygotes by crossing wild-type males to *daf-21(nr2081)/nT1 n754* hermaphrodites and then crossing non-Unc male progeny to *daf-21(p673)* hermaphrodites. Non-dauer hermaphrodite progeny were picked individually and transferred to new plates each day for 3 days and were then used for PCR assays of *nr2081*. Three heterozygotes were obtained and in each case the progeny at 20° were similar. A total of 16% arrested as L1 or L2 larvae, 70% formed dauers, and 14% developed as non-dauers ($n = 161$).

To create worms with the genotype *daf-21(p673)/daf-21(p673)/+*, we used *ctDp11*, a free duplication containing part of chromosome V (including *daf-21*, *her-1*, and *unc-42*) and part of chromosome III (including *dpy-17*, *ncl-1*, and *unc-36*). We crossed *dpy-17 ncl-1 unc-36; him-8; her-1 unc-24; ctDp11* males to *dpy-17 ncl-1 unc-36; daf-21(p673)* hermaphrodites. We picked wild-type progeny [*dpy-17 ncl-1 unc-36 him-8/+; her-1 unc-42 +/+ + daf-21(p673); ctDp11*] and allowed them to self-fertilize. In the next generation, we picked non-Dpy non-Unc dauers (*dpy-17 ncl-1 unc-36; daf-21; ctDp11*) and then chose strains that segregated no males [*him-8(+)*]. To assay the Daf-c phenotype at 20°, we let parents carrying the duplication (*p673/p673/+*) lay eggs overnight and scored the progeny after 3 days. We found 7.2% of the progeny formed dauers ($n = 568$), in contrast to progeny of *daf-21(p673)/+* mothers, which never form dauers.

PCR, DNA sequencing, and DNA oligonucleotides: Sequencing was performed by the ABI dye terminator cycle sequencing method (Perkin-Elmer, Norwalk, CT) using either AmpliTaq DNA polymerase or AmpliTaq DNA polymerase FS. The PCR products were analyzed by the University of Washington Biochemistry and Pharmacology DNA Sequencing Facilities and by Axy's Pharmaceuticals. PCR and sequencing primers were obtained from various sources, and sequences of all listed primers are available on request.

Molecular identification of *daf-11*: *daf-11(m597)* was isolated by P. Albert and D. Riddle from a strain with active transposition of Tc1. Southern blots of genomic DNA from outcrossed *m597* strains were probed with Tc1 DNA, and a 0.38-kb *NdeI* fragment was found to contain a 1.6-kb Tc1 insertion that cosegregated with *m597* in recombinants. Genomic DNA from *daf-11(m597)* was digested with *NdeI* and used for nested inverse PCR with Tc1 primers, and the products were ligated at low concentration to encourage intramolecular ligation. The PCR primers for the first round were oriented outward from the ends of Tc1 (OLG34 and OLG35). The primer for the second round (OLG23) is derived from the inverted repeat sequence at the ends of Tc1 and also oriented outward. The resulting PCR product was cloned into pBluescript II KS⁺ (Stratagene, La Jolla, CA) that had been digested with *EcoRI* and treated with Klenow to generate blunt ends to create plasmid pTJ277. We verified that pTJ277 contained DNA flanking the *m597* Tc1 by using it as probe on Southern blots of genomic DNA from *m597*, from four phenotypic revertants of *daf-11(m597)*, and from genetic recombinants that retained *m597* but removed most of the rest of the Tc1-mutagenized chromosome V. In each case, polymorphisms were detected consistent with a Tc1 insertion only in the *daf-11(m597)* strains.

Determination of the *daf-11* cDNA sequence: pTJ277 was used as a probe to isolate genomic and cDNA phage. Five

phages with overlapping genomic inserts were isolated at a frequency of 1.8×10^{-4} from the Stratagene λ FIXII genomic library. Sequence analysis was performed on subclones from one of these phages to determine part of the *daf-11* genomic sequence. This sequence was also compared to that generated by the *C. elegans* Sequencing Consortium (1998), which sequenced the region containing *daf-11* during the course of this work. *daf-11* corresponds to the predicted gene B0240.3. From $\sim 10^6$ plaques from one cDNA library (A. Fire, personal communication) and 3×10^5 plaques from another (Barstead and Waterston 1989), one *daf-11* clone was recovered. This cDNA insert was subcloned into pBluescript II using the *KpnI* and *SacI* sites in the flanking phage DNA to create plasmid pTJ342, which was sequenced. Since this cDNA appeared incomplete on both ends, an additional 9×10^5 plaques from a mixed-stage *C. elegans* cDNA library (Stratagene) were probed with a 2.4-kb *Clai-HindIII* genomic fragment containing most of the cyclase domain. One *daf-11* cDNA clone was recovered, and its insert was excised into pBluescript II using helper phage K07, to generate plasmid pTJ584. On the basis of the presence of a poly(A) tail, pTJ584 appears complete at the 3' end, and it was sequenced to determine the 3' untranslated region (UTR) and exon boundaries at the 3' end of the gene. *daf-11* mRNA sequence at the 5' end was determined from reverse transcriptase-PCR (RT-PCR) products generated with the GIBCO-BRL (Gaithersburg, MD) 5' RACE system (Frohman *et al.* 1988). Mixed-stage RNA for the RT-PCR procedure was isolated either by the method of D. Pilgrim (personal communication) or essentially by the method of Miller *et al.* (1988). The 5' end was isolated in two pieces, one with primers from the coding region and the most 5' segment with a gene-specific primer and a primer to the *C. elegans* splice leader SL1. Sequencing of bulk RT-PCR product was performed on exons 1, 8, 9, 10, and parts of 2, 7, and 11. This sequence showed no evidence of a mixed population of cDNA. cDNA sequence from the rest of the gene was based on only one cDNA for each section, so alternative splicing cannot be ruled out for these regions.

Determination of *daf-21* cDNA sequence: The 5.8-kb *BamHI* insert in pEM1 was used as a probe to isolate cDNA phage from a mixed-stage *C. elegans* cDNA library (Stratagene). Approximately 3% of plaques hybridized to this probe that contains C47E8.4 and *daf-21/Hsp90*. The inserts for 12 positive plaques were excised into pBluescript II using helper phage K07. On the basis of restriction digest with *EcoRI*, we found that 11 of the 12 were clearly related. We sequenced the longest, pEM29, with gene-specific primers designed on the basis of the Genefinder (P. Green, personal communication) prediction for the Hsp90 coding sequence. This analysis confirmed all of the intron-exon splicing predictions and revealed a 3' untranslated region of at least 117 bp. Our analysis of 12 publicly available 3' expressed sequence tags showed that the five most extensive sequences end at the same point as pEM29, suggesting this is the true 3' end of the mRNA. We did not find evidence of a poly(A) tail. The 5' end of pEM29 is exactly at the predicted ATG start codon. To determine the true 5' end of *daf-21*, we used the GIBCO-BRL 5' RACE system for RT-PCR (Frohman *et al.* 1988). Mixed-stage RNA was isolated as above. A *daf-21*-specific primer (OLG 344) was used for first strand cDNA synthesis, and the 5' end was amplified with a second *daf-21*-specific primer (OLG367) and an SL1-specific primer (OLG193). Sequencing of the RT-PCR product showed a 5' untranslated leader of 4 bp between the SL1 spliced leader and the *daf-21* ATG.

Sequence of *daf-11* and *daf-21* mutations: DNA was amplified by PCR from total genomic DNA (Wood 1988) or from lysed worms, and bulk PCR products were sequenced. Mutations were sequenced on both strands with gene-specific primers.

For *daf-11(m87)*, *daf-11(p169)*, and *daf-11(sa203)* only the coding region of the cyclase domain was sequenced. For *daf-11(sa195)*, all coding sequence upstream of the nonsense mutation was sequenced, and for *daf-11(m84)* the entire coding sequence was determined. For *daf-21(p673)* the genomic sequence spanning the entire coding region was sequenced. For *daf-21(nr2081)*, only the region immediately adjacent to the deletion was sequenced.

Modification of Genefinder predictions of *gcy* genes: We analyzed the Genefinder predictions for *gcy-1* to *gcy-18*, all of the TM-GC genes fully sequenced at the time. The GCY-1 through GCY-18 proteins and a selected set of previously reported TM-GCs were subjected to an initial multiple alignment with CLUSTALW 1.4. We manually inspected the resulting alignments for regions in which specific Genefinder-predicted proteins appeared to have deletions of conserved sequence or insertions of unconserved sequence in a conserved region. Typically, these stood out dramatically in a multiple alignment, and all but one occurred precisely at Genefinder-predicted exon-intron boundaries. In these cases, we manually scanned genomic sequence for splice sites that would produce clearly improved alignments. In four cases, such an alternative splice was found. F23H12.6 (GCY-13) had an anomalous insertion of VSRHNP after predicted amino acid (aa) 614; use of a splice donor 21 nucleotides (nt) upstream (2215 nt from the predicted ATG, splice junction sequence AGT ^ GTGAGTC) precisely eliminated the anomaly. F23H12.6 (GCY-13) also had an anomalous deletion of 10 amino acids (following the F23H12.6 predicted sequence FFSDVVGFT); use of a splice donor 30 nt downstream (4495 nt from the predicted ATG, splice junction sequence CAG ^ GCGAGTT) added 10 amino acids (VLANKSTPLQ) that restored typical similarity to other TM-GCs. [This alteration is questionable because it requires the use of an unusual splice donor sequence. To test the validity of this change, we performed a BLASTP search of the nr GenBank data set with an 18-amino-acid sequence (VGFTVLANKSTPLQVVNL) centered on the inserted 10 amino acids. All 34 hits with *P* values <0.9 were TM-GCs.] ZK455.2 (GCY-9) had an anomalous insertion of VCKLRQKII after predicted aa941, which was precisely removed by using a splice donor 27 nt upstream (4742 nt from the predicted ATG, splice junction sequence CAG ^ GTTTGCC). B0024.6 (GCY-6) had an anomalous insertion of 18 amino acids (RKIF QKSTNISSFFHLFS) after predicted aa1161 that was precisely removed by creating a new 54-nt intron (starting 5798 nt from the predicted ATG, splice donor sequence AAC ^ GTAAAT and splice acceptor sequence GTTTCAG ^ CTG). While this approach to amending Genefinder predictions is not rigorous and may have ignored some errors, we think it highly likely that the revised protein predictions more closely approximate the true structures. As a partial test of validity we performed TBLASTN searches (default parameters), using as the query the protein most closely related to the gene under analysis. This permits detection of conserved protein coding regions in a manner independent of Genefinder predictions. In each case, the TBLASTN match to the target gene verified our exon assignment.

The *gcy* names for TM-GCs correspond to cosmid names from the *C. elegans* Sequencing Consortium as follows (see also Yu *et al.* 1997): *daf-11* = B0240.3; *gcy-1* = AH6.1; *gcy-2* = R134.2; *gcy-3* = R134.1; *gcy-4* = ZK970.5; *gcy-5* = ZK970.6; *gcy-6* = B0024.6; *gcy-7* = F52E1.4; *gcy-8* = C49H3.2; *gcy-9* = ZK455.2; *gcy-10* = *odr-1* = R01E6.1; *gcy-11* = C30G4.3 (missing TM domain; see text); *gcy-12* = F08B1.2; *gcy-13* = F23H12.6; *gcy-14* = ZC412.2; *gcy-15* = ZC239.7; *gcy-16* = F27H7.c; *gcy-17* = W03-F11.2; *gcy-18* = ZK896.8; *gcy-19* = C17F4.6; *gcy-20* = F21H7.9; *gcy-21* = F22E5.3; *gcy-22* = T03D8.5; *gcy-23* = T26C12.4; *gcy-24* = W03F11.2; *gcy-25*:Y105C5B.a; *gcy-26* = ZK896.8; *gcy-27* =

C06A12.4. For completeness, we also assigned names to the seven predicted soluble guanylyl cyclases as follows: *gcy-31* = T07D1.1; *gcy-32* = C06B3.8; *gcy-33* = F57F5.2; *gcy-34* = M04G-12.3; *gcy-35* = T04D3.4; *gcy-36* = C46E1.2; *gcy-37* = C54E4.3.

8-Bromo-cGMP assays: Plates (2 cm) were filled with 2 ml NGM agar (Wood 1988) with 8-bromo-cGMP (Sigma, St. Louis) added to a given concentration from a freshly made 250 mM stock. The next day, a fresh overnight stock of *Escherichia coli* OP50 in Luria broth (LB) was harvested and resuspended at 5% (w/v) in sterile H₂O. Twenty microliters of this bacteria was spotted onto each plate and allowed to dry for a few hours. Eight to 20 gravid hermaphrodites were picked on and allowed to lay eggs at room temperature for up to 3 hr and then removed. These plates, generally containing 50–120 eggs, were placed in a sealed box at 25°. Since 8-bromo-cGMP reduced growth synchrony, plates grown at 25° were scored at various times, generally several times for each plate, between 36 and 52 hr after egg laying. Since 8-bromo-cGMP induced dauer recovery in *daf-11(sa195)* dauers (data not shown), one set of experiments was scored particularly frequently to be certain that the drug blocks dauer formation rather than inducing rapid recovery. In all experiments, obvious dauers, L3s, or older animals were removed at each inspection and counted; the remaining L1 and L2 animals were left to continue growth. At the end of 52 hr, animals that were still L1s or L2s were scored as arrested. The frequency of dauer formation was based only on the dauers, L3s, and older animals and was averaged across all similar assay plates. For most data points, more than 100 worms were counted and assays were performed on at least 2 different days. The following were exceptions: one *daf-8* intermediate concentration and *daf-11(m87)* 1.25 mm assays (done only 1 day each) and *daf-8* 2.5 mm assay (45 worms). 8-Bromo-cAMP (Sigma) assays were done in the same manner.

In several 8-bromo-cGMP assays, many animals arrested as L1 or L2 larvae or formed larvae with only some characteristics of dauers. We interpret this to mean that 8-bromo-cGMP can affect non-dauer development as well as execution of the dauer developmental program. These animals generally constituted <25% of the total, and they were excluded from the data presented. The following were exceptions to this low frequency: *daf-11(m87)* 0.6 mm 8-bromo-cGMP (34% not counted); *daf-11(sa195)* 1.25 and 2.5 mm 8-bromo-cGMP (about 40% not counted); *daf-21(p673)* 1.25, 2.5, and 5 mm 8-bromo-cGMP (about 50% not counted); *daf-4(e1364)* 5 mm 8-bromo-cGMP (42% not counted); *daf-8(e1393)* 2.5 and 5 mm 8-bromo-cGMP (about 50% not counted); *daf-2(e1370)* 5 mm 8-bromo-cGMP (62% not counted); *tax-4(ks11)* 5 mm 8-bromo-cGMP (67% not counted); *tax-4(p678)* 5 mm 8-bromo-cGMP (43% not counted). Conclusions based on these data were essentially unchanged if the partial-dauer animals were counted as dauers.

Construction of *daf-11::gfp* fusions: The 4.2 kb upstream of *daf-11* plus the entire genomic coding region was cloned in two pieces from PCR products generated from the *daf-11*-containing cosmid W04E7. Taq polymerase was mixed 100:1 with Pfu polymerase to reduce the mutation rate (after Barnes 1994). Primers were designed with restriction enzyme sites to facilitate cloning. OLG376 (*Xma*I site added) and OLG378 (*Xho*I site added) were used to amplify the 5' part and OLG377 (*Xma*I site added) and OLG363 (*Bam*HI site added) were used to amplify the 3' part. OLG376 and OLG377 each changed two nucleotides in intron 6 to produce the *Xma*I site used in cloning. Sequential cloning of these two PCR products joined them at the shared *Xma*I site to reconstruct the *daf-11* genomic structure. This fragment was subcloned into the *Sa*II and *Bam*HI sites of pPD95.70 to make pTJ642, an in-frame fusion of a nuclear localization signal and green fluorescent protein (GFP) to the DAF-11 C terminus, and into pPD95.79 to gener-

ate pTJ643, a similar fusion without a nuclear localization sequence (NLS). A shorter translational *daf-11::gfp* fusion was generated by cloning a single PCR product (primers OLG311 and OLG310) into the *NsiI* and *BamHI* sites of pPD95.67 to create pTJ536. A. Fire, S. Xu, J. Ahnn and G. Seydoux (personal communication) provided all of the fusion vectors.

Construction of *daf-21* subclones: We constructed subclones of T10E3, a *daf-21* rescuing cosmid, by digesting it with either *BamHI*, *PstI*, or *StuI* and shotgun cloning fragments into pBluescript SK⁺ (Stratagene). One fully rescuing subclone (pEM1) was recovered, which contained a 5.8-kb *BamHI* fragment. pEM1 was digested with *XmaI* and a 3.7-kb fragment (shown in Figure 5) extending from the insert *XmaI* site to the vector *XmaI* site was subcloned into pBluescript SK⁺ to create pEM12.

Construction and analysis of transgenic worms: *daf-11* transgenics were generated by injection (Mello *et al.* 1991) of *lin-15(n765)* animals, using a *lin-15* rescuing plasmid (pbLH98 at 60 ng/ μ l) as a transformation marker (Huang *et al.* 1994). The concentrations of key experimental DNAs were: full-length *daf-11::gfp* fusion (pTJ643) at 200 ng/ μ l, and *daf-11* (*exon 5*):*gfp* fusion (pTJ536) at 50 ng/ μ l. We also analyzed a full-length *daf-11::nls-gfp* fusion (pTJ642), injected at 200 ng/ μ l, which gave nuclear-localized patterns that were otherwise similar to the non-NLS fusion. For pTJ643, injected *daf-11(sa195)*; *lin-15(n765)* animals were grown at 20° for 1 day and then transferred to 25° and screened for non-Muv (*lin-15*-rescued) or non-Daf (*daf-11*-rescued) progeny. For Figure 3E, GFP expression was analyzed in two independent lines containing the full-length, NLS construct [JT8903 *lin-15(n765)*; *saEx237* and JT8904 *lin-15(n765)*; *saEx238*]. Animals were grown at 25° to enable identification of transgenic animals. GFP expression was observed using epifluorescence microscopy and fluorescent cells were identified by Nomarski microscopy on the same animal. Photographs were taken on Kodak Elite II slide film (ISO 400) and were digitally formatted. Adobe Photoshop was used to adjust brightness and contrast, add annotation, and convert color to gray scale.

For analysis of pheromone effects on GFP expression in *daf-11* mutants, *lin-15(n765)*; *saEx238* or *daf-11(sa195)*; *saEx289* animals were grown on 50–80 μ l of pheromone at 25° as described (Thomas *et al.* 1993), conditions sufficient to induce over 90% dauer formation in the wild type. GFP expression in L1 larvae was observed 1 day after eggs were laid, and dauers were counted and assayed for GFP expression 2 days after eggs were laid.

daf-21 transgenics were generated similarly except that the dominant *rol-6(su1006dm)* marker (pRF4, 200 ng/ μ l) was used as the marker. *daf-21(p673)* mutants have few progeny and injections in this background yielded few transformants, so we injected into the wild type with cosmids (5 ng/ μ l, individually or in pools) or plasmid subclones (15 or 20 ng/ μ l). We then crossed the heritable transgenic arrays into a *daf-21(p673)* background. We used a linked, visible marker to follow *daf-21* in crosses because maternal rescue prohibited scoring the Daf-c phenotype in the progeny of *daf-21/+* mothers. *lon-3 daf-21/+* males were crossed to transgenic Rol hermaphrodites (*saEx**), and Rol cross-progeny were allowed to self-fertilize. From plates that segregated Lons, we identified strains of the genotype *lon-3 daf-21*; *saEx**. We found that the Lon phenotype is best scored in adults, when it largely suppresses the Rol phenotype. Therefore, in these strains there are Rol larvae, and most of the adults are Lon non-Rol. In all cases, some dauers segregated indicating that *daf-21(p673)* must be homozygous. To assay rescue, we determined the frequency of dauer formation in synchronous larval populations grown uncrowded at 25°. Strains with full rescue had only 10–30% dauers, strains with partial rescue had 40–50% dauers, and strains with no rescue had >80% dauers.

Rescue of dauer formation and dauer recovery by *saEx289*:

Plates were prepared and assayed as for 8-bromo-cGMP assays (above), except that 80 μ l of M9, pheromone solution, or a mixture (0, 10, or 20 units of pheromone) were added. Eggs were laid at room temperature for 3 hr and then plates were shifted to 25°. Dauers and L3 or older animals were counted and all L3 or older animals were removed once or twice per day starting at 48 hr. At 96 hr the number of dauers remaining on the plate was counted. The percentage of dauer formation was calculated as $100 \times (\text{no. of dauers}) / (\text{total no. of worms})$ at 48 hr, and the percentage of recovery was calculated as $100 \times (\text{total no. of recovered animals}) / (\text{total no. of recovered animals} + \text{dauers left on plate at 96 hr})$. Dauers that crawled up the side of the plate were not counted, as they did not have a chance to recover. Each data point was repeated on at least 2 days and on four to nine plates.

Chemotaxis assays: Assays of chemotaxis to NaCl were performed as described (Bargmann and Horvitz 1991b) except that worms were allowed to swim for 15–30 min on a chemotaxis plate without attractant between the last wash and the assay. This step allowed the worms to better acclimate to the assay conditions and led to more reproducible results (C. Bargmann, personal communication). Volatile avoidance assays with 2-nonanone were performed as described (Troemel *et al.* 1997) except that worms were washed three times with S basal and once with water. Worms were grown and assays were performed at 20°. Because a large fraction of *daf-11* mutant animals form dauers at 20°, *daf-12* double mutants were assayed, with a *daf-12* single mutant as control (as in Vowels and Thomas 1994).

Mosaic analysis: Four gravid adults of genotype *dpy-17(e164) ncl-1(e1865) unc-36(e251); daf-11(sa195); ctDp11* were placed on a plate at 25°. Three days later, non-Unc dauer mosaics were identified either visually or (in most cases) by flooding the plate with 1% SDS and picking animals that were alive and thrashed (1% SDS kills non-dauers and Unc dauers did not thrash). Mosaics were inspected by Nomarski microscopy, and cells were assayed for the presence or absence of the duplication by observing the Ncl (enlarged nucleolus) phenotype of several amphid cells. It was sometimes not possible to unambiguously identify all amphid neurons in each animal. In most cases, ASI, ADL, ASK, ASE, ASH, AWC, AUA, and ASJ neurons on each side were analyzed, and often several other cells were also analyzed.

Identification of the *daf-21(nr2081)* deletion mutation: A library of mutagenized worms was screened by PCR with nested primers (Liu *et al.* 1999) to identify a *daf-21* deletion called *nr2081*. The primers were C47E8.5 F1 (5' ATTCGTAATTC GACCCTGC), C47E8.5 R1 (5' TTCTGTAGATGCGGGAA GCG), C47E8.5 F2 (5' TGCCAAATGAATCAAGCGGC), and C47E8.5 R2 (5' AAGCGTGAGATTGTGGCTCCTC) and resulted in a 2844-bp band in wild type. A mutant with a smaller band was identified, and sequencing of the mutant band showed an 860-bp deletion plus a 3-bp insertion. This mutation is predicted to remove amino acids 32–287 and to add 94 novel amino acids from another reading frame. To follow *nr2081* in crosses, we used three primers, two that span the deletion and one within the deletion. Together these primers resulted in diagnostic bands for the mutant and wild type that could be scored simultaneously in heterozygotes.

RESULTS

***daf-11* encodes a transmembrane guanylyl cyclase:** We cloned *daf-11* using *m597*, a transposon-tagged allele isolated from a strain with active Tc1 transposition (kindly provided by P. Albert and D. Riddle). Southern

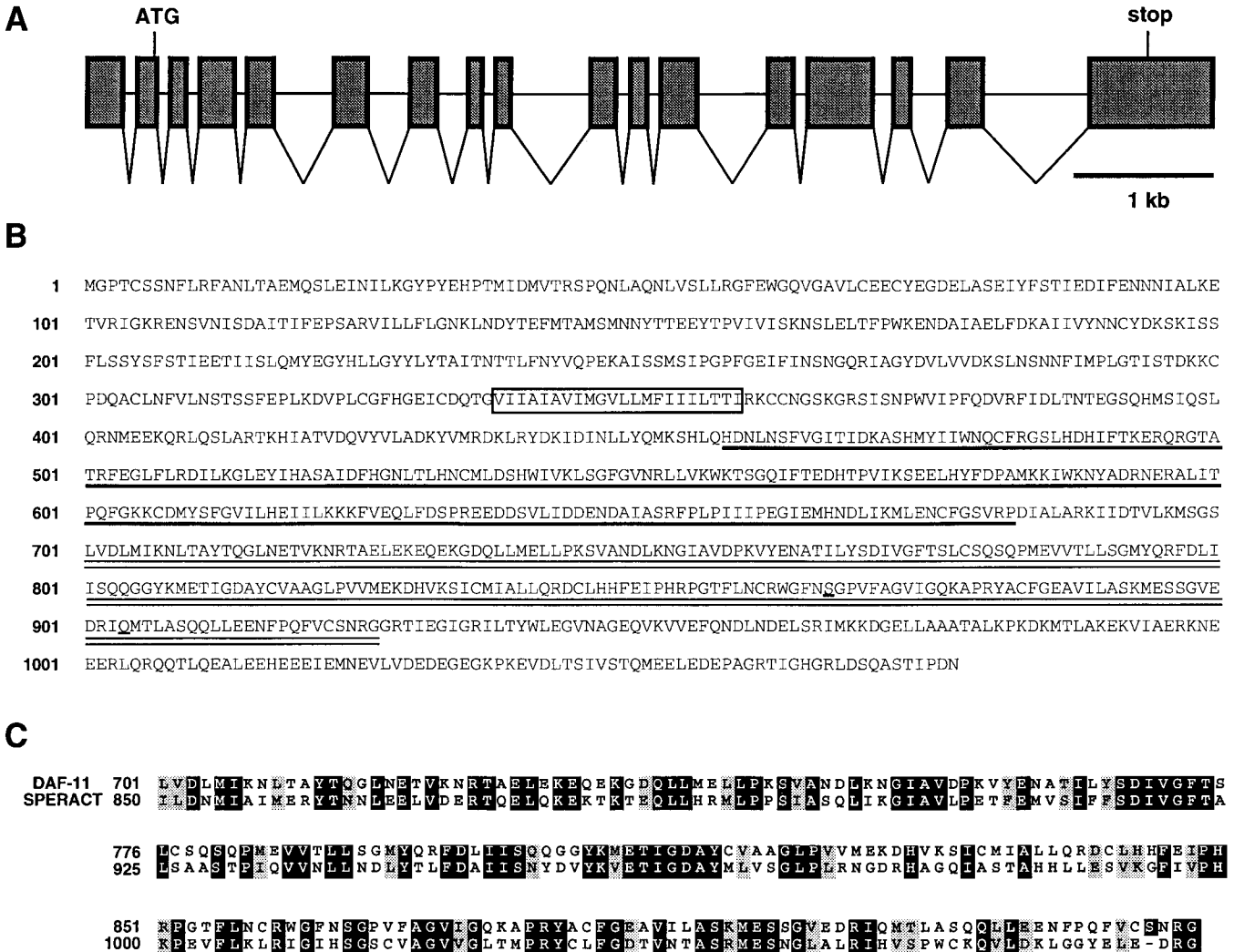


Figure 1.—The DAF-11 protein and homology to transmembrane guanylyl cyclases. (A) Splicing pattern of the *daf-11* mRNA, as determined by comparison of genomic DNA sequence to cDNA sequence. (B) Predicted DAF-11 protein sequence. The putative transmembrane domain is boxed, the kinase homology domain is underlined, and the guanylyl cyclase domain is underlined twice. (C) Alignment of the guanylyl cyclase domain of DAF-11 and its closest relative outside of *C. elegans*, the sea urchin speract receptor (accession no. p16065).

blot analysis revealed a Tc1 insertion present in strains containing *m597* and absent in recombinants and revertants not containing *m597* (data not shown). We cloned genomic DNA flanking this Tc1 insertion by inverse PCR and used the flanking DNA to isolate phages from cDNA and genomic DNA libraries. The two *daf-11* cDNAs isolated were both incomplete, but together permitted determination of the last 3 kb of the poly(A)-terminated *daf-11* mRNA. We completed sequence at the 5' end of the mRNA from RT-PCR products. We also determined genomic sequence for most of the gene from subclones of genomic phage. The Genome Sequence Consortium completed the sequence of this region during the course of our work. Comparison of the genomic sequence to the cDNA sequence indicated that the *daf-11* mRNA contains 17 exons and spans almost 8 kb of genomic DNA (Figure

1A). The mRNA contains one long open reading frame predicted to encode a 1077-amino-acid protein that is a member of the TM-GC family (Figure 1, B and C).

Transmembrane guanylyl cyclases catalyze the production of cyclic GMP from GTP and have been identified in animals from *C. elegans* to humans (reviewed in Yuen and Garbers 1992; Drewett and Garbers 1994). They function in various signal transduction systems including a chemotaxis response in sea urchin sperm, regulation of blood pressure by natriuretic peptides, and visual signaling in mammals. TM-GCs consist of an N-terminal extracellular domain, a single transmembrane domain, and an intracellular region. The intracellular region contains a domain with homology to protein kinases (KHD, *kinase homology domain*) and a C-terminal GC domain that catalyzes the conversion of GTP to cGMP. The KHD lacks key residues required for kinase

catalytic activity (Yuen and Garbers 1992). The DAF-11 protein contains each of these characteristic domains (Figure 1B). As is true of most TM-GCs, strong DAF-11 homology to other guanylyl cyclases is restricted to the KHD and cyclase domains. An alignment of the cyclase domain of DAF-11 and its closest relative outside of *C. elegans*, the sea urchin speract receptor, is shown in Figure 1C. The speract receptor and DAF-11 share 22% identity and 47% similarity in the KHD and 43% identity and 64% similarity in the cyclase domain.

We used BLAST searches (Altschul *et al.* 1990) to identify other guanylyl cyclase-related genes in the nearly complete *C. elegans* genome sequence (*C. elegans* Sequencing Consortium 1998). As of 10/99, these searches had identified a total of 28 *C. elegans* genes that are clearly related to TM-GCs. The 27 TM-GC genes other than *daf-11* were named *gcy-1* through *gcy-27* (similar to *guanylyl cyclase*). Corresponding names from the *C. elegans* Genome Project are described in materials and methods and by Yu *et al.* (1997). On the basis of our analysis of *daf-11* and the fact that GFP fusions to several other *gcy* promoters are expressed in chemosensory neurons (Yu *et al.* 1997), it seems likely that most of the *C. elegans* TM-GCs are involved in chemosensory signal transduction processes.

Seven other genes were identified with higher similarity to soluble guanylyl cyclases (not shown). Since over 95% of all *C. elegans* genes are included in this analysis (J. Sulston and R. Waterston, personal communication), these observations suggest that all *C. elegans* guanylyl cyclases fall into one of these two previously defined families. Distinguishing between the TM and soluble GCs was straightforward based both on degree of identity in the cyclase domain and other structural features of each class of proteins.

Sequence changes in *daf-11* mutants: *daf-11* alleles vary in their phenotypic effects (Thomas *et al.* 1993; Vowels and Thomas 1994). To determine the specific effects of *daf-11* mutations on protein function, we sequenced PCR products generated from mutant genomic DNA. Identified mutations are indicated in Figure 1B. Of the known *daf-11* mutations, three of the sequenced alleles (*m597*, *sa195*, and *m87*) confer the strongest defects, consistent with a strong loss-of-function or null phenotype: a strong Daf-c phenotype at 25° but not at 15°, chemotaxis defects to nonvolatile and some volatile attractants, and severely defective dauer recovery at all temperatures (Vowels and Thomas 1994). *sa195* is a nonsense mutation at Q450, which is predicted to truncate DAF-11 before the KHD and the cyclase domains; it is the best candidate for a *daf-11* molecular null allele. *m597* results from a Tc1 insertion in the KHD, in the codon I518. *m87* is a missense mutation in the cyclase domain that changes S866 to F in a highly conserved region (Figure 1, B and C). A fourth allele, *p169*, has a missense mutation that changes the highly conserved G867 to R in the cyclase domain. The dauer phenotypes

of the *p169* mutant are consistent with a strong loss-of-function allele (strong Daf-c at 25°, weak Daf-c at 15°, poor dauer recovery), but other phenotypes have not been tested.

Two other *daf-11* alleles confer unusual phenotypes. The *daf-11(sa203)* mutant was strongly Daf-c at 25°, but also formed 88% dauers at 15° ($N = 234$). *sa203* has a nonsense mutation at Q904, just at the end of the conserved residues of the cyclase domain (Figure 1, B and C). We speculate that the *sa203* mRNA expresses a truncated protein product that interferes with the function of another protein. Alternatively, a second undetected mutation may be responsible for the unusual phenotype. The *daf-11(m84)* mutant is also unusual: it is very strongly Daf-c at both 15° and 25°, the dauers recover much more quickly and efficiently than do other *daf-11* mutants, and *m84* adults have only weak defects in response to the volatile attractant isoamyl alcohol (Vowels and Thomas 1994). For each of these pheno-

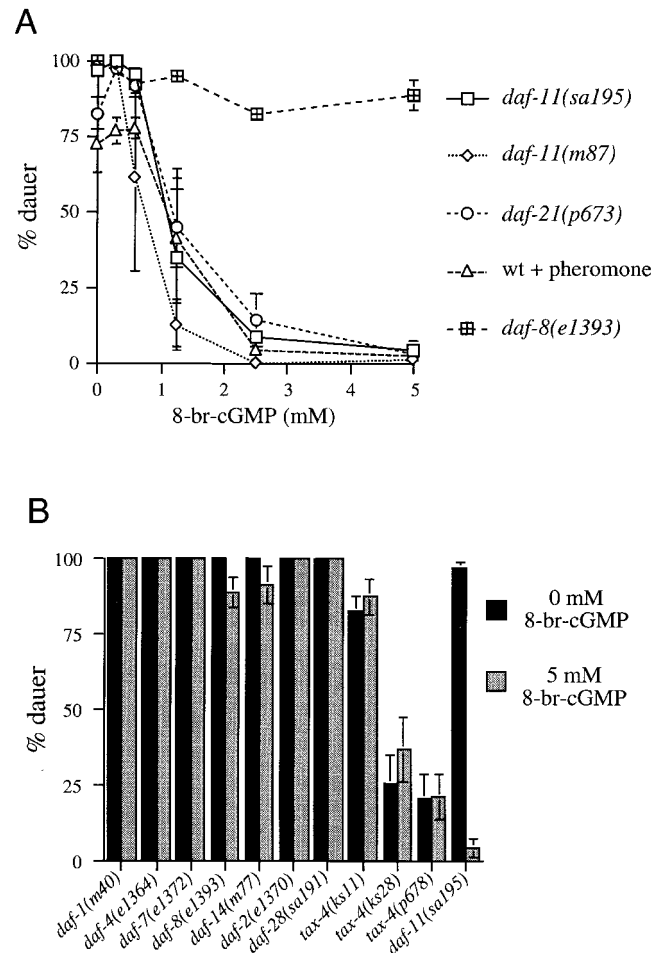


Figure 2.—Effects of 8-bromo-cGMP on dauer formation. (A) Dose response curve for *daf-11*, *daf-21*, and *daf-8* mutants at 25° and on the wild type with pheromone. (B) Effect on other Daf-c mutants at 25°. Data for *daf-11(sa195)* and *daf-8(e1393)* animals are the same as in A and are shown for comparison. Bars indicate standard errors of the mean.

types, the unusual *daf-11(m84)* phenotypes are still seen when *in trans* to the strong alleles *m87* and *sa195*. *m84* is slightly dominant to the wild-type allele for its dauer formation phenotype (Vowels and Thomas 1994). These data suggest that the *m84* mutation affects only some of the functions of DAF-11, and that it may encode a protein that interferes with the function of other proteins. *daf-11(m84)* causes a G806 to E change, affecting an unconserved residue in a relatively conserved part of the cyclase domain (Figure 1, B and C).

cGMP signaling is perturbed in *daf-11* and *daf-21* mutants: To test the biological relevance of the DAF-11 sequence homology to TM-GCs and to test directly for a role for cGMP in chemosensation, we assayed the effect on dauer formation of the membrane permeant cGMP analogue 8-bromo-cGMP (Figure 2A). If the *daf-11* mutant phenotype is due to a loss of guanylyl cyclase activity, supplementing with 8-bromo-cGMP might suppress the Daf-c phenotype. When grown at 25° with plentiful food without 8-bromo-cGMP, over 95% of *daf-11(sa195)* and *daf-11(m87)* animals formed dauers. In contrast, when 5 mM 8-bromo-cGMP was added to the growth medium, <1% formed dauers. Intermediate concentrations of the drug caused intermediate suppression of the Daf-c phenotype. 8-Bromo-cGMP similarly suppressed pheromone-induced dauer formation in the wild type in a dose-dependent manner, directly implicating cGMP in normal dauer formation.

We hypothesized that 8-bromo-cGMP suppressed dauer formation *daf-11* mutants by substituting for the cGMP normally synthesized by the DAF-11 protein. This hypothesis predicts that 8-bromo-cGMP would not suppress mutations in genes that act downstream of or in parallel to *daf-11*. As predicted, we found that 8-bromo-cGMP did not prevent constitutive dauer formation in mutants for *daf-1*, *daf-4*, *daf-7*, *daf-8*, *daf-14*, *daf-2*, or *daf-28* (Figure 2B). On the basis of gene interactions, it is thought that all of these genes act downstream of or in parallel to *daf-1* (Riddle *et al.* 1981; Thomas *et al.* 1993; Gottlieb and Ruvkun 1994; Malone *et al.* 1996). In contrast, 8-bromo-cGMP fully suppressed the Daf-c phenotype of *daf-21(p673)* (Figure 2A, and see below). To test whether this suppression is specific to cGMP, we tested the response of *daf-11*, *daf-21*, *daf-1*, *daf-4*, *daf-7*, *daf-14*, *daf-2*, and *daf-28* mutants to 8-bromo-cAMP. At 5 mM, 8-bromo-cAMP caused developmental arrest in the wild type, but 0.5 mM 8-bromo-cAMP allowed normal growth and had no effect on dauer formation in any of the Daf-c strains (data not shown). These results implicate cGMP in dauer formation and provide direct evidence that DAF-11 functions *in vivo* as a guanylyl cyclase.

***daf-11* expression in sensory neurons controlling dauer formation and dauer recovery:** To identify cells in which *daf-11* is expressed, we constructed a fusion gene containing 4.2 kb upstream of *daf-11* and the entire genomic coding region with GFP (Chalfie *et al.* 1994) fused at the C terminus. A transgenic array containing this construct (*saEx289*) rescued the Daf-c phenotype

of *daf-11(sa195)* animals (Figure 3E). All GFP-expressing cells were amphid neurons, as identified by comparison to the known positions and processes of all neurons (White *et al.* 1986). GFP expression was visible in the ciliated sensory endings, as expected, as well as in the cell bodies and dendrites (Figure 3). In some adults, expression was seen only in the ciliated endings (Figure 3, C and D) and the cell bodies (not shown), indicating that within the dendritic compartment the protein is preferentially localized to the ciliated endings. The expression pattern we observed was generally consistent with phenotypic evidence for *daf-11* function in specific sensory pathways, as discussed below and summarized in Figure 3E.

The GFP fusion protein was reproducibly expressed in the amphid neuron classes ASJ and ASI, both implicated in regulating dauer formation. Constitutive dauer formation in *daf-11* mutants is dependent on the function of the ASJ neurons (Schackwitz *et al.* 1996), and expression of *daf-11::gfp* in ASJ neurons supports a model in which the DAF-11 guanylyl cyclase acts in ASJ to regulate dauer pheromone response. A simple possibility is that cGMP produced by DAF-11 inhibits the dauer-promoting activity of ASJ neurons, thus preventing dauer formation, and that dauer pheromone or *daf-11* mutations reduce the cGMP level, activating the ASJ neurons and inducing dauer formation.

In contrast to the ASJ neurons, the ASI neurons function together with another neuron class, ADF, to repress dauer formation in the absence of dauer-inducing conditions (Bargmann and Horvitz 1991a; Schackwitz *et al.* 1996). Various results suggest that ASI neurons repress dauer formation by secreting DAF-7, a TGF- β related protein (Bargmann and Horvitz 1991a; Thomas *et al.* 1993; Ren *et al.* 1996; Schackwitz *et al.* 1996). Expression of *daf-11::gfp* in ASI was unexpected, since genetic evidence supports a *daf-11* function that acts in parallel to *daf-7* (Thomas *et al.* 1993; Schackwitz *et al.* 1996). Several explanations might reconcile these findings. First, one of the many other TM-GCs that have been identified in *C. elegans* (above; Yu *et al.* 1997) may function in ASI neurons redundantly with the DAF-11 TM-GC, thus masking a role for *daf-11* in ASI neurons. Second, it is possible that *daf-11* function in ASI neurons is unrelated to dauer formation. Third, expression of *daf-11::gfp* in ASI could be an artifact of our assay: an unexpectedly large fraction of *gfp* fusions to neuronally expressed genes show expression in ASI neurons (Troemel *et al.* 1995; D. A. Birnby, E. M. Link, J. J. Vowels, H. Tian, P. L. Colacurcio and J. H. Thomas, unpublished data). As an independent approach to testing *daf-11* function in dauer formation, we undertook mosaic analysis of *daf-11(sa195)*. Unfortunately, analysis of several putative mosaics from over 250,000 animals screened (see materials and methods) led to only two conclusions. First, *daf-11(sa195)* is very slightly dominant in the strain used for mosaic analysis, complicating interpretation of mosaic losses. Second, loss of *daf-11*

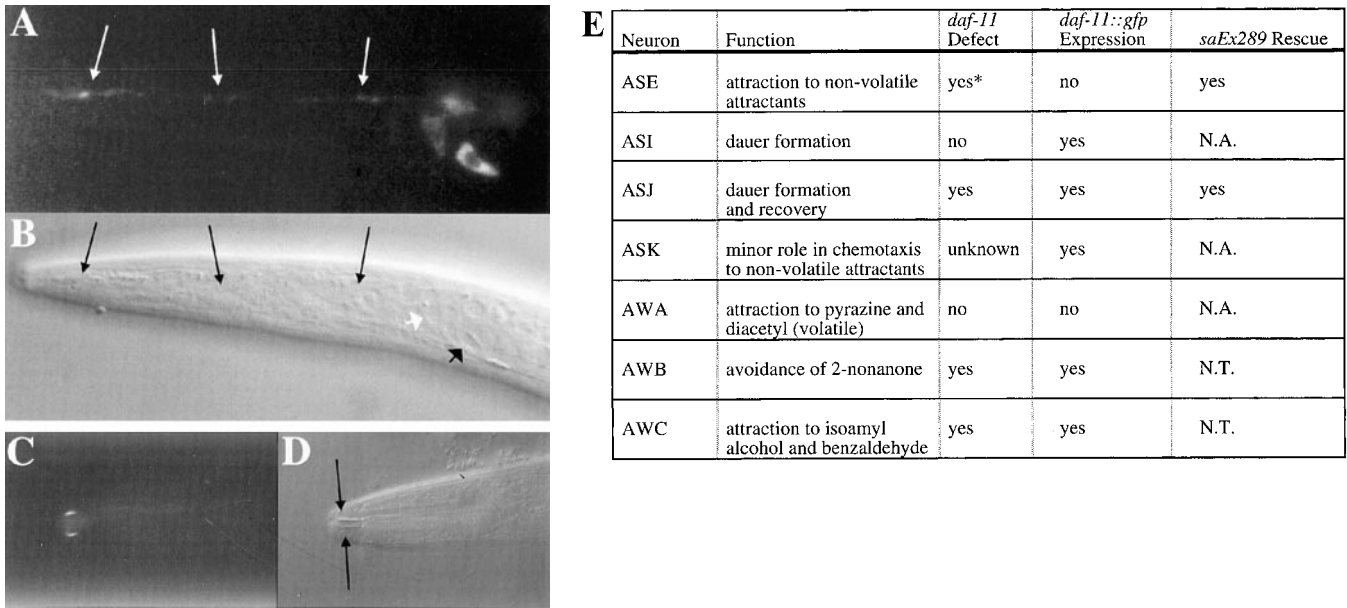


Figure 3.—Expression of *daf-11::gfp* fusion transgene. (A and B) Fluorescence (A) and Nomarski (B) images of an L1 animal. Arrows in A and B point to the same locations. Expression is seen in the dendrites of amphid neurons (long arrows), in an AWC cell body (short white arrow in B), and an ASJ cell body (brightest spot toward the right in A and short black arrow in B). ASI and ASK (seen in A) are out of the plane of focus. (C and D) Fluorescence (C) and Nomarski (D) images of an adult. Arrows in D point to the sites of fluorescence in C, which are sensory cilia. Expression was also in the cell body (not shown). All photographs are of strain JT9386. (E) With the full length *daf-11::gfp* fusion, expression was observed in all cells listed, though infrequently in AWB. The short (fifth exon) *daf-11::gfp* fusion was expressed only in AWB, AWC, ASI, and ASK. NA, not applicable; NT, not tested.

in any of several amphid neurons (including the ASJ class) slightly increased the likelihood of dauer formation, with no clear pattern of critical cells (data not shown). Taken together with previous studies (Schackwitz *et al.* 1996), these results suggest that *daf-11* function in preventing dauer formation may be primarily in ASJ neurons, but that *daf-11* also acts in other cells.

Under appropriate environmental conditions, dauers recover and resume their normal life cycle (Cassada and Russell 1975). Cell-kill experiments show that ASJ is the only amphid neuron class essential for this recovery (Bargmann and Horvitz 1991a). Strong *daf-11* mutants are severely defective in recovery from the dauer state (Vowels and Thomas 1994). We hypothesized that *daf-11* might function in ASJ neurons to promote dauer recovery. To test this hypothesis, we assayed expression of *daf-11::gfp* in dauers that were induced by dauer pheromone at 25°. Expression in ASJ of the rescuing fusion array *saEx238* was analyzed in 13 dauers (26 cells). We saw definite expression in ASJ in 6 cells and expression in 12 more cells whose positions were consistent with ASJ. The arrangement of neurons in the dauer larva is somewhat different from that in the well-described L1 larva, and positive identification was not always possible. These results show that *daf-11* is expressed in ASJ neurons in most or all dauers and is consistent with a function of DAF-11 in ASJ neurons to promote recovery from the dauer state.

The dauer-inducing pheromone does not affect *daf-*

11::gfp: Exposing animals to the dauer-inducing pheromone strongly reduces expression of *daf-7::gfp* fusions, suggesting that the effects of the pheromone on this TGF- β pathway are mediated at the level of *daf-7* expression (Schackwitz *et al.* 1996; Ren *et al.* 1996). In contrast, exposure to dauer pheromone had no effect on expression of a full-length *daf-11::gfp* fusion in any cells (data not shown), suggesting that pheromone affects this pathway at a level other than *daf-11* transcription. Since 8-bromo-cGMP suppresses the Daf-c phenotype of *daf-11* mutants and blocks the dauer-inducing effects of the pheromone in wild-type larvae, dauer pheromone presumably reduces cGMP levels in *daf-11*-expressing neurons. It is possible that pheromone directly inactivates DAF-11 guanylyl cyclase activity, perhaps by binding to the extracellular domain. However, given the pleiotropy of *daf-11* mutations, this is an unlikely general model for *daf-11* function. We favor a model in which pheromone regulates cGMP levels indirectly, by binding an unidentified receptor or receptors and initiating a transduction process that ultimately stimulates a cGMP phosphodiesterase or reduces DAF-11 guanylyl cyclase activity. A phosphodiesterase is involved in cGMP-mediated visual transduction in mammals, where it is activated by light to lower cGMP levels in rod outer segments (Miki *et al.* 1975).

***daf-11* expression in cells regulating chemotaxis and 2-nonanone avoidance:** *daf-11::gfp* expression was also seen in AWC and ASK neurons (Figure 3E). The AWC

class is required for chemotaxis toward the volatile attractants isoamyl alcohol and benzaldehyde. Since *daf-11* mutants are defective in response to these attractants, expression in AWC neurons was predicted. There is evidence that the ASK neurons play a minor role in chemotaxis to lysine and possibly other nonvolatile attractants (Bargmann and Horvitz 1991b). The ASK class may also play a small part in promoting dauer formation in response to pheromone (Schackwitz *et al.* 1996). *daf-11* may function in ASK neurons in one of these responses. Expression in AWC and ASK was variable, which may indicate lower levels of *daf-11* expression in these neurons or may result from incomplete regulatory sequences in the transgene.

A shorter *daf-11* fusion construct, with the same promoter region plus only the first 136 codons of *daf-11* (up to the fifth exon) fused to *gfp*, was expressed consistently in the AWC and AWB neurons and was expressed occasionally in the ASI and ASK neurons (Figure 3E). (Another transgenic array containing the same construct had consistent expression in ASI neurons, but the strain stopped expressing detectable GFP before quantitative data were collected.) Reinspection of strains carrying the full-length *daf-11* fusion also revealed occasional expression in AWB cells. Presumably the differences in expression among fusions result from internal *daf-11* regulatory sequences, but we have not further investigated this. The AWB neurons are required for avoidance of the repulsive compound 2-nonanone (Troemel *et al.* 1997), prompting us to test this response in *daf-11* mutants. To facilitate growth, the strains tested also contained a *daf-12* mutation to prevent dauer formation, and the *daf-12* single mutant was tested as a control (see materials and methods). We found that both *daf-11(sa195)* and *daf-11(m84)* mutants are defective in response to either undiluted or a 10⁻¹ dilution of 2-nonanone (Figure 4). Together these results indicate a role for *daf-11* in AWB sensory transduction.

In addition to their other phenotypes, *daf-11* mutants are defective in chemotaxis toward nonvolatile chemicals, a process mediated primarily by the ASE neurons. However, *daf-11::gfp* expression in ASE cells was only rarely seen in larvae bearing the longer fusion and was never seen (0/21 cells) in adults grown at 20° (the temperature at which chemotaxis assays are performed). This lack of expression could be because the fusion lacks regulatory sequences or because the effect of the *daf-11* mutation on chemotaxis is not mediated through ASE. We found that the longer fusion could partially rescue the *daf-11* chemotaxis defect (Figure 3E), supporting the idea of an ASE-independent effect of *daf-11* on chemotaxis. However, *daf-11::gfp* expression is weak and variable in some cells and it remains possible that a low level of *daf-11* expression in ASE neurons was not identified by our reporter assay.

***daf-21* encodes an Hsp90:** Genetic analysis has indi-

cated that *daf-21* acts at the same step as *daf-11* in the dauer formation pathway (Thomas *et al.* 1993), and *daf-11* and *daf-21(p673)* mutants have nearly identical defects in sensing odorants (Vowels and Thomas 1994). Furthermore, the suppression of the *daf-21(p673)* Daf-c phenotype by 8-bromo-cGMP suggests that the *daf-21(p673)* mutation, like *daf-11* mutations, reduces cGMP levels. Therefore, we also cloned the *daf-21* gene. We genetically mapped *daf-21* with respect to three cloned genes (see materials and methods) and used the genetic distances to infer an approximate physical position for *daf-21* (Figure 5A). We used transformation rescue with cosmids and cosmid subclones to localize *daf-21* to a 5.8-kb genomic fragment that fully rescues the Daf-c phenotype of *daf-21(p673)* (Figure 5, B and C). The *C. elegans* Sequencing Consortium (1998) predicted two divergently transcribed genes in this interval: C47E8.4 and C47E8.5, which encodes the *C. elegans* heat-shock protein 90. Two lines of evidence indicate that *daf-21* corresponds to the Hsp90 gene. First, a subclone (pEM12) that contains the Hsp90 coding region and about 1 kb of upstream sequences partially rescues the *daf-21* Daf-c phenotype, despite lacking >70% of the C47E8.4 coding region (Figure 5C). Second, by

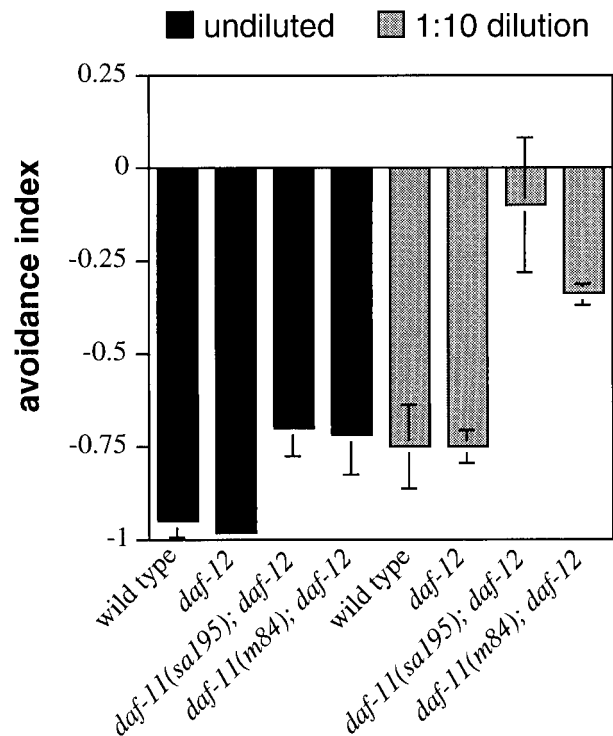


Figure 4.—Avoidance of the volatile repellent 2-nonanone. Response of wild type, *daf-11; daf-12* double mutants and the *daf-12* single mutant control. The *daf-12(m20)* allele was used in all cases. Response is calculated as [(no. of worms in the third of the plate containing 2-nonanone) – (no. of worms in the third of the plate opposite to the 2-nonanone)] / (total no. of worms). A strong avoidance response is –1. Each data point is the average of two to four assays with >300 worms total. Bars indicate the standard deviation among assays.

sequencing *daf-21(p673)* genomic DNA, we identified a missense mutation in the Hsp90 coding region. This mutation changes E292 to K, a dramatic charge change in a highly conserved amino acid that is likely to affect protein function (Figure 5D and Figure 6).

Hsp90 proteins consist of two highly conserved domains connected by a charged linker region (reviewed in Scheibel and Buchner 1998; Buchner 1999). Both the N-terminal and C-terminal domains contain chaperone sites (Young *et al.* 1997; Scheibel *et al.* 1998). The N-terminal domain includes an ATP-binding pocket and

a cleft that is large enough to accommodate polypeptides (Prodromou *et al.* 1997a,b; Stebbins 1997). ATP binding is required for Hsp90 function (Obermann *et al.* 1998; Grenert *et al.* 1999) and induces peptide dissociation from the N-terminal domain (Scheibel *et al.* 1998). The charged linker varies in length from 0 amino acids in *E. coli* to 50 amino acids in humans. This charged region enhances binding of the amino-terminal domain to denatured protein and mediates an effect of bound peptide on ATP affinity (Scheibel *et al.* 1999). The C-terminal domain binds promiscuously to par-

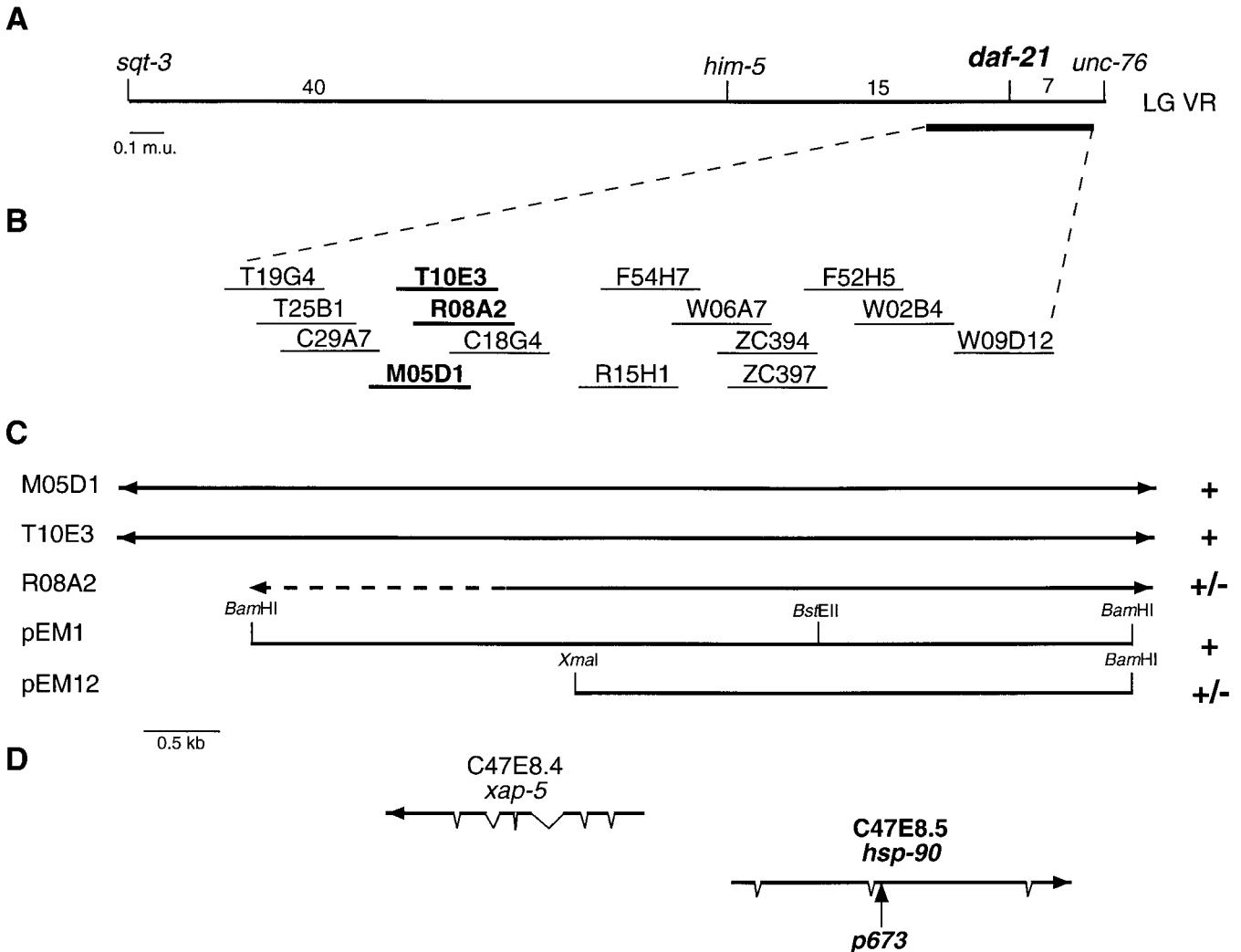


Figure 5.—Cloning the *daf-21* gene. (A) Genetic mapping of *daf-21(p673)*. A portion of linkage group V is shown with the relative positions of three markers for which the genes have been previously cloned (van der Keyl *et al.* 1994; Bloom and Horvitz 1997; Pennington and Meneely, personal communication). The number of recombinants (Sqt non-Unc and Unc non-Sqt) that we identified in each interval is shown. (B) Cosmid rescue of *daf-21*. A region of overlapping cosmids surrounding the predicted location of *daf-21* is shown (Waterston *et al.* 1997). The cosmids in boldface type are shown in more detail in C. (C) Part of the overlapping region of the rescuing cosmids is shown. Arrows indicate that the cosmids extend beyond the region depicted. Although the precise left endpoint of R08A2 is unknown, it is somewhere in the dotted part of the line. M05D1 and T10E3 rescued *daf-21(p673)* (one and three lines, respectively) and R08A2 gave intermediate rescue (three lines). The restriction sites used to create the two subclones pEM1 (5.8 kb) and pEM12 (3.7 kb) are shown. pEM1 rescued fully (two lines) and pEM12 rescued partially (one line). (D) The predicted genes in this region are shown aligned with the genomic subclones above in C. Arrows indicate the direction of transcription. The bold segments represent exons and the thinner lines represent introns. The arrow points to the location of the *p673* mutation.

tially folded proteins in an ATP-independent manner (Scheibel *et al.* 1998) and is required for Hsp90 dimerization (Nemoto *et al.* 1995; Meng *et al.* 1996; Nemoto and Sato 1998). The *C. elegans* Hsp90 protein includes all of these domains (Figure 6), and the E292K change in *p673* affects an early amino acid in the C-terminal domain.

In vertebrates, there are two Hsp90 cytoplasmic isoforms, α and β . In addition there is a third cytosolic relative, Trap-1/Hsp75, that lacks the charged region (Chen *et al.* 1996; Song *et al.* 1996). A fourth Hsp90 relative called GRP94/GP96 is found in the endoplasmic reticulum. DAF-21/Hsp90 is 74 and 76% identical to human Hsp90 α and Hsp90 β , respectively, and is clearly most closely related to these proteins (Figure 6). There are no other predicted *C. elegans* genes with this degree of similarity to Hsp90, indicating that there is a single *C. elegans* Hsp90 ortholog. However, there are predicted *C. elegans* genes orthologous to Trap-1/Hsp75 (R151.7) and GRP94/GP96 (T05E11.3; Figure 6). Hsp90 is a highly abundant protein whose expression is increased further under conditions of stress. Consistent with abundant expression, we and others have identified

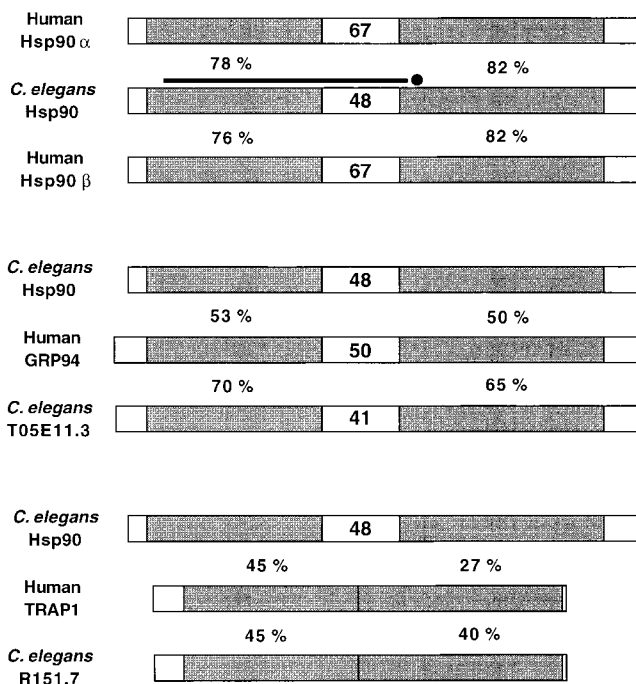


Figure 6.—The Hsp90 protein family. Selected members of the Hsp90 protein family are represented as boxes. The two shaded regions in each protein are the conserved N-terminal (left) and C-terminal (right) domains. The number of amino acids in the charged linker region between the two domains is indicated. The percent identity between pairs of proteins is shown for both the N-terminal and C-terminal domains. In the upper representation of DAF-21, the location of the E292K mutation in *daf-21(p673)* is shown by the black circle, and the extent of the deletion in *daf-21(nr2081)* is shown by the heavy line. Protein sequences were aligned using the ClustalW program in MacVector (Oxford Molecular Group).

many *daf-21*/Hsp90 cDNAs (Waterston *et al.* 1992; W. R. McCombie, J. M. Kelley, L. Aubin, M. Goscochea, M. G. FitzGerald, A. Wu, M. D. Adams, M. Dubnick, A. R. Kerlavage, J. C. Venter and C. A. Fields, personal communication; Y. Kohara, H. Mitsuki, A. Nishigaki, T. Motohashi, A. Sugimoto and H. Tabara, personal communication). Approximately 3% of clones in a mixed stage cDNA library hybridized to the pEM1 rescuing subclone. It is intriguing that previous studies showed *daf-21*/Hsp90 transcription is elevated in dauers (Dalley and Gomb 1992), though this is unlikely to explain the *daf-21(p673)* Daf-c phenotype. Sequencing of a cDNA and RT-PCR products confirmed the predicted intron-exon structure and showed that the mRNA is *trans*-spliced to the *C. elegans* spliced leader SL1.

***daf-21(p673)* is not a loss-of-function mutation:** It is known from genetic studies in yeast and *Drosophila* that Hsp90 is required for viability (Borkovitch *et al.* 1989; Cutforth and Rubin 1994; van der Straten *et al.* 1997). In contrast, *daf-21(p673)* mutants have an assortment of sensory defects and reduced fertility, but otherwise grow nicely in the laboratory. We investigated whether *daf-21(p673)* is a loss-of-function mutation by testing *daf-21(p673)* *in trans* to three deficiencies that delete the gene. We crossed *Df/+* males to *daf-21(p673)* homozygous hermaphrodites. If *p673* were a loss-of-function allele, we would expect that the *daf-21(p673)/Df* progeny would form dauers or display some more severe phenotype such as larval arrest (if *p673* were a partial loss-of-function allele enhanced by the *Df*). However, we found that the *daf-21(p673)/Df* animals were perfectly viable and did not form dauers (Table 1). This result indicates that two copies of *daf-21(p673)* are required for the Daf-c phenotype and suggests that the Daf-c phenotype is not due to loss of *daf-21* function. The deficiencies did have obvious effects on the *daf-21(p673)* phenotype, however. *daf-21(p673)* homozygotes have reduced fertility (Vowels 1994), and this phenotype was enhanced by the deficiencies such that the *daf-21(p673)/Df* heterozygotes are nearly sterile at 25°. In addition, although *daf-21(p673)/+* animals never have dauer progeny, ~40% of *daf-21(p673)* homozygotes from *daf-21(p673)/Df* mothers form dauers at 20°. These results also confirm that the deficiencies delete the *daf-21* gene, as expected from genetic map data. We conclude that *daf-21(p673)* is not a simple loss-of-function mutation and that dosage of the mutant allele is important in determining the phenotype.

To determine the null phenotype of *daf-21*, we obtained a deletion mutation kindly provided by Axyx Pharmaceuticals, NemaPharm Group. The mutant was isolated according to the method of Liu *et al.* (1999; see materials and methods) and contained an 860-bp deletion plus a 3-bp insertion. This mutation is predicted to remove amino acids 32–287 and to add 94 novel amino acids from another reading frame. *daf-*

TABLE 1
Summary of *daf-21* phenotypes

Genotype	Phenotype
<i>p673/p673</i>	Strong Daf-c, reduced fertility
<i>p673/+</i>	Wild type
<i>p673/p673/+</i>	7% Daf-c, good fertility
<i>p673/Df</i>	Non-Daf-c, nearly sterile
<i>nr2081/nr2081</i>	L2 to L3 larval lethal
<i>nr2081/+</i>	Wild type
<i>p673/nr2081</i>	70% Daf-c, some lethality

21(nr2081) deletion homozygotes arrested growth at the L2 to L3 larval stages (Table 1), indicating that Hsp90 is essential in *C. elegans*, as it is in yeast and *Drosophila* (Borkovitch *et al.* 1989; Cutforth and Rubin 1994; van der Straten *et al.* 1997). To confirm that *p673* and *nr2081* are allelic, we examined *daf-21(p673)/daf-21(nr2081)* heterozygotes. We found that these animals have many (70%, $n = 161$) dauer progeny at 20°, indicating that these mutations fail to complement for the dauer-constitutive phenotype. Of the remaining progeny, about half arrested as L1 or L2 larvae and about half developed as non-dauers. We note that in combination with *daf-21(p673)*, the *daf-21(nr2081)* deletion mutation has a stronger effect on dauer formation than any of the three large deficiencies tested, suggesting that the deficiencies delete other genes relevant to dauer formation.

Though gain-of-function mutations most often display some degree of dominance, *daf-21(p673)* is recessive in the sense that *daf-21(p673)/+* heterozygotes never form dauers. We tested for weak dominance by using a duplication to create animals with three copies of the *daf-21* locus (see materials and methods). While *daf-21(p673)/+* mothers made 0% dauer progeny at 25°, *daf-21(p673)/daf-21(p673)/+* mothers grown in parallel made approximately 7% dauer progeny (Table 1). We conclude that two copies of the *daf-21(p673)* allele probably result in a stronger mutant phenotype, consistent with the model that *daf-21(p673)* is a weak gain-of-function mutation.

DISCUSSION

A variety of shared mutant phenotypes suggest that the *C. elegans* genes *daf-11* and *daf-21* act at the same step to regulate chemosensory transduction in several of the exposed, ciliated amphid neurons. First, mutations in both genes cause defects in chemotaxis to the nonvolatile attractants Cl^- , cAMP, and biotin (Vowels and Thomas 1994), responses controlled primarily by the ASE neurons with lesser contributions from the ADF, ASG, and ASI neurons (Bargmann and Horvitz 1991b). Second, *daf-11* and *daf-21* mutants are defective in response to the volatile attractants isoamyl alcohol

and benzaldehyde (Vowels and Thomas 1994), behaviors that require the AWC neurons (Bargmann *et al.* 1993). A third shared phenotype is constitutive dauer formation, a developmental process normally regulated by the environment (Riddle *et al.* 1981; Thomas *et al.* 1993). This dauer-constitutive phenotype is suppressed in both *daf-11* and *daf-21* mutants by killing the dauer-promoting neurons ASJ, suggesting that this phenotype results from activation of the ASJ neurons (Schackwitz *et al.* 1996). In addition, mutations that disrupt the sensory cilia have been used in epistasis experiments to demonstrate that the dauer-constitutive phenotype in *daf-11* and *daf-21* mutants requires intact ciliated sensory endings, suggesting that these genes play a role in an early step of chemosensory signal transduction (Vowels and Thomas 1992). Other Daf-c genes function in a TGF- β -like signaling pathway or in an insulin-like signaling pathway, but these are distinct from *daf-11* and *daf-21* because their Daf-c phenotypes are not dependent on the ASJ neurons or on structurally normal sensory cilia (Vowels and Thomas 1992; Thomas *et al.* 1993; Gottlieb and Ruvkun 1994; Schackwitz *et al.* 1996).

***C. elegans* dauer formation provides a genetic model for TM-GC function in sensory transduction:** In addition to *daf-11*, several other genes are candidates for functioning in sensory transduction events controlling dauer formation. A model for this transduction process is provided by mammalian visual transduction, in which a TM-GC (RetGC) is known to function (reviewed in Koutalos and Yao 1993; Hurley 1987). In this pathway, the heterotrimeric G-protein transducin mediates activation of a cGMP phosphodiesterase in response to light (Baehr *et al.* 1982). Two G-protein α subunits, *gpa-2* and *gpa-3*, are implicated in dauer formation. Loss-of-function mutations in these genes cause a Daf-d (*dauer formation defective*) phenotype, and animals carrying activated *gpa-2* or *gpa-3* transgenes have a Daf-c phenotype (Zwaal *et al.* 1997). *gpa-3::lacZ* is expressed in amphid neurons that regulate dauer formation, and the Daf-c phenotype of animals carrying an activated *gpa-3* transgene is suppressed by defects in the ciliated endings of the amphid neurons (Zwaal *et al.* 1997). These findings are consistent with a role for *gpa-3* analogous to that of transducin in visual transduction. However, loss of *gpa-3* function weakly suppresses the Daf-c phenotype of *daf-11(m47)* (Zwaal *et al.* 1997), suggesting that *gpa-3* functions either downstream of or in parallel to *daf-11*. Thus the relationship between these genes and *daf-11* is unclear. A putative cyclic nucleotide phosphodiesterase (F26A1.14) has been identified by the *C. elegans* Sequencing Consortium (1998), but it is not yet known whether this gene is involved in dauer formation.

In visual transduction, cGMP acts directly on an excitatory cyclic nucleotide gated ion channel (Fesenko *et al.* 1985). In *C. elegans*, *tax-4* and *tax-2* have recently been shown to encode α and β subunits of a cyclic

nucleotide gated ion channel (Coburn and Bargmann 1996; Komatsu *et al.* 1996). A *tax-4::gfp* fusion is expressed in the amphid neurons ASK, ASI, ASG, ASE, AFD, AWC, and ASJ (Komatsu *et al.* 1996), a set that includes four of the five neurons in which *daf-11::gfp* fusions are expressed, and *tax-4* mutants have a weak dauer-constitutive phenotype (Coburn *et al.* 1998). If TAX-4 is a target of cGMP synthesized by DAF-11, the Daf-c phenotype of *tax-4* mutants should not be suppressed by growth on 8-bromo-cGMP. As predicted, we found that 8-bromo-cGMP had no effect on dauer formation in *tax-4* mutants (Figure 3B). In contrast to *tax-4* mutants, *tax-2* mutants do not form dauers even at 27° (data not shown), a condition that induces dauer formation more strongly than 25° (M. Ailion, personal communication; Malone *et al.* 1996). However, *tax-2* mutants are weaker than *tax-4* mutants in many respects (Coburn and Bargmann 1996), so this does not rule out a role for *tax-2* in dauer formation.

This genetic model system can be used to determine *in vivo* the functions of the three domains of the TM-GC molecule as well as the relationships among the components of a cGMP transduction pathway. Mutations already exist in many of these genes and gene disruptions could be generated in the phosphodiesterase and in other potential components discovered by sequence analysis (Zwaal *et al.* 1993; Liu *et al.* 1999). These mutants could be used to analyze the functional relationships among these genes in the control of dauer formation. In addition, animals carrying *daf-11* transgenes mutated in specific domains or amino acids can be generated and analyzed in a *daf-11* null background. The combination of these techniques will generate a better understanding of the role of transmembrane guanylyl cyclase signaling *in vivo*.

The KHD of the transmembrane-guanylyl cyclase gene family: We analyzed the sequence of 14 of the *C. elegans* TM-GC genes in more detail (all the genes with complete sequence at the time of the analysis). With the exception of DAF-11, all of our protein sequence analysis was done with gene products predicted by the Genefinder program (P. Green, personal communication), with minor amendments described in materials and methods. Thirteen of the 14 analyzed TM-GCs have the standard TM-GC structure, a transmembrane domain separating a large extracellular domain from the intracellular kinase homology and cyclase domains. The one exception, GCY-11, is quite similar to other TM-GCs except that it appears to lack a predicted transmembrane domain. Since this difference might be due to a Genefinder error or *gcy-11* might be a pseudogene, it was not further analyzed.

Though all previously reported TM-GCs have large extracellular domains, these domains are highly divergent from one another and in most cases a function has not been identified. Two features of the *C. elegans* genes nevertheless suggest that these extracellular do-

ains consistently have important functions. First, 27 of the 28 *C. elegans* genes in the completed genome sequence are predicted to have a large extracellular domain of similar size. Second, a limited amount of homology is apparent in this domain between nearly all of the *C. elegans* TM-GCs and those of other organisms. This ranges as high as 28% identity between GCY-12 and the Drosophila DrGC-1 (McNeil *et al.* 1995), but is usually restricted to a few short regions that may represent shared structural elements. We hypothesize that the sequence divergence among TM-GC extracellular domains reflects binding of divergent ligands rather than a lack of functional significance.

The sequencing of a large set of divergent TM-GCs affords important new insight into the conserved features of the kinase homology domain. An alignment of the KHD of the 13 analyzed *C. elegans* proteins and 5 from other organisms is shown in Figure 7, with annotations showing the blocks of conservation observed in *bona fide* protein kinases (Hanks *et al.* 1988). Although the KHD is related to protein kinases, nearly all members of the TM-GC family, including the new members from *C. elegans*, lack key amino acid residues required for kinase catalytic activity (Hanks *et al.* 1988; Yuen and Garbers 1992; Figure 7 legend), indicating that this domain does not have kinase activity. Importantly, the ATP-binding domain found in all kinases is clearly not conserved in the KHD of TM-GCs (Domain I, Figure 7). Previous reports that the KHDs of specific TM-GCs have weak but significant similarity to kinase ATP-binding domains (Singh *et al.* 1988; Chinkers *et al.* 1989) are not supported by our comparison of TM-GCs as a group (Figure 7). This observation potentially confounds interpretation of data that ATP affects cyclase activity (Chinkers *et al.* 1991; Parkinson *et al.* 1994). For example, ATP appears to protect the enterotoxin receptor cyclase from inactivation (Vaandrager *et al.* 1993a,b) and ATP potentiates the effects of the ligand ANP on GC-A (Chinkers and Garbers 1989). On the basis of our results with DAF-21/Hsp90, we speculate that these effects are mediated by ATP-Hsp90 interactions with TM-GCs.

Some conserved regions of the guanylyl cyclase KHD are not particularly conserved in true protein kinases, especially C-terminal to block III and N-terminal to block I (Figure 7). These facts suggest that the KHD diverged from true protein kinases before the divergence of known TM-GCs from one another. Despite the differences between protein kinases and the KHD of TM-GCs, there is a clear general parallel between their most conserved stretches (Figure 7). These parallels in sequence conservation indicate that the TM-GC and protein kinase groups have been subject to related selective pressure. We speculate that this conservation reflects selection for a common protein binding domain rather than enzymatic kinase activity. One possible binding partner for this domain is DAF-21/Hsp-90.

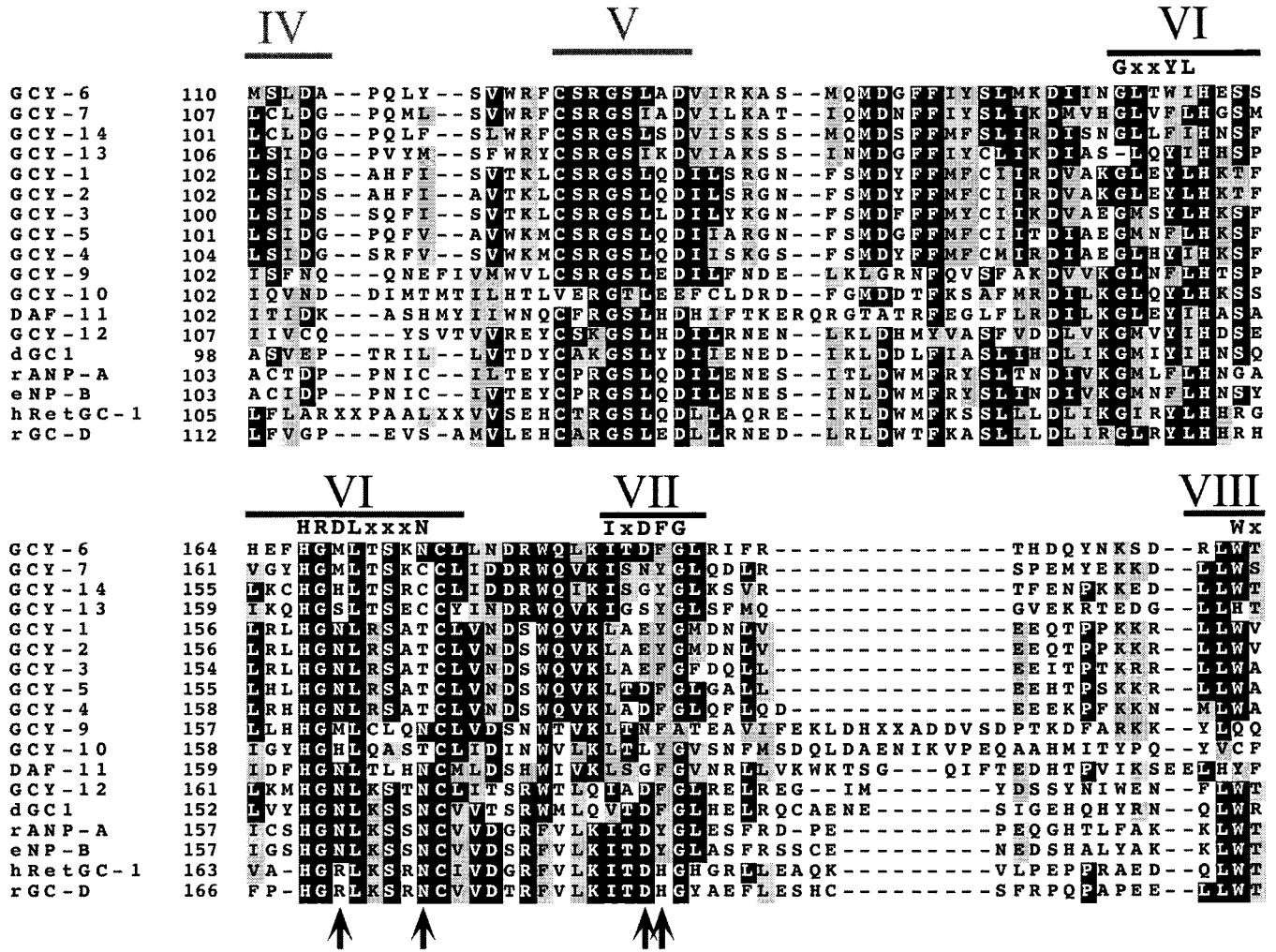


Figure 7.—Continued.

1044 bp upstream of the Hsp90 translation start site. To confirm the gene assignment, we identified an E292 to K change in the Hsp90 coding region in the *daf-21(p673)* mutant. Finally, we identified a deletion predicted to severely truncate the Hsp90 protein and showed that it fails to complement *daf-21(p673)*.

In other organisms, Hsp90 is reported to be one of the most highly expressed proteins (1–2% of total). In accord with this, we found that ~3% of *C. elegans* cDNA clones hybridized to an Hsp90 probe. Surprisingly, reduction of Hsp90 expression to 5% of normal was shown to have little effect in *Saccharomyces cerevisiae* (Picard *et al.* 1990; Xu and Lindquist 1993). We speculate that the maternal rescue of the *daf-21(p673)* mutant phenotypes is a consequence of high levels of Hsp90 protein or RNA contributed to the developing egg by the mother, combined with tolerance for greatly reduced levels of Hsp90 function.

A possible role of Hsp90 in chemosensory transduction: Although Hsp90 function is not entirely understood, two related functions have been ascribed to this chaperone protein (reviewed in Scheibel and Buch-

ner 1998; Buchner 1999; Caplan 1999; Mayer and Bukau 1999). First, it is believed that Hsp90 is important for refolding denatured or misfolded proteins. In an *in vitro* assay, Hsp90 prevented the irreversible aggregation of denatured proteins and promoted refolding (Weich *et al.* 1992). As for all heat-shock proteins, Hsp90 expression is induced upon heat shock (Welch and Feramisco 1982; Jakob *et al.* 1995; Freeman and Morimoto 1996; Schumacher *et al.* 1996), consistent with this general role in handling unfolded proteins. In *C. elegans*, transcription of Hsp90 is increased 15-fold in dauers compared to non-dauers (Dalley and Golomb 1992), providing additional chaperone activity under the stressful conditions that dauers are capable of enduring. Hsp90 plays a second role in the absence of stress by stably binding to specific target proteins and helping them to achieve their mature structures. Typically, the Hsp90-bound target protein is inactive but capable of being activated, and Hsp90 then dissociates from the target protein upon its activation (reviewed in Scheibel and Buchner 1998; Buchner 1999; Caplan 1999; Mayer and Bukau 1999). There is no evidence that

VIII

IX

		APE		DxWSFG
G CY - 6	209	SPELRLRTDDILG-----SRE--		GDVYSLFGITSAELITRSSVFDLENRKEDA-EEI
G CY - 7	206	APELRLRAEDIK-----SKE--		GDVYSLFGITCAELITRKGVMEDRKEDEP-EEI
G CY - 1 4	200	PPENLRNENEER-----LPE--		GDVYSLFGITCSEILTRSSAFDLENRKEKPD-VVI
G CY - 1 3	204	APEVLRREGLTSG-----TQA--		GDVYSLFSGIVCSSELVGHSSAWNLNENRKEEA-DEI
G CY - 1	201	APEVLRGSLSVS-----QMEPSAD		YSFATIASEILTKKEAWDILDRKEDC-EEI
G CY - 2	201	APEVLRGSLSVS-----QMEPSAD		YSFATIASEILTKKEAWDILDRKEDC-EG-
G CY - 3	199	APEVLRGSLTVS-----QMDPSAD		VSFATIASEILTRKEAWDLKERKEGY-DEI
G CY - 5	200	APEVLRGSLTIH-----QMDPSAD		VSFATIASEILTKKEAWDISNRKEGA-DEI
G CY - 4	204	APEVLRGSLSIE-----QMDSSAD		YSFATIAVASEILTKKEAWDLRRKE---EI
G CY - 9	215	APEIIREIVTTKTIP-----EGSQSAD		IYALGMVLYQILFRVPEPFHERNKSINK-LME
G CY - 1 0	216	FPEHIREYDDSGKQP---RVVVRGSPKGD		IYCVGMIFYMMVEREDPYHLIHSVLRP-NAT
DAF - 1 1	216	DPAMKKIWKNYADRNERALITPQFGKKCD		MYVSGVILHEIILKFKFVEQLFDSPREEDDS
G CY - 1 2	211	APEAMTINGSLAISN-----PPTPKAD		VYAFGIIFHEIFTRREGPYKIYVQXKKK-DSV
dGC 1	200	APELRLRNHIHGS-----QK--		GDVYAFATIMYEIFSRKGE---PFGQINFEP-KEI
rANP - A	216	APELRLMASPPA-----RGSQA		GDVYSLFGIILQEIALRSGVFYVEGLDLS-KEI
eNP - B	217	APELRLTYDRHPP-----QGTQK		GDVYSLFGIILQEIALRNGPFYVDMGLSP-KEI
hRetGC - 1	212	APELRLDPALER-----RGTLAG		DVYSLAIIIMQEVVCRSA---PYAMDLTLP-EEI
rGC - D	215	APELRLRGRPGWPG-----KATFK		GDVYSLFGIILQEVLTRDP---PYCSWGLSA-EEI

X

XI

				L	PxxRP
G CY - 6	257	IYMLKKGGLQ---SPRPSLE-HDESIEIN		PALLHLVLRDCWTERPSPSERPDIKQVASQLRSM	
G CY - 7	254	IYLLKKGGLK---SPRPDL-EYDHTIEIN		PALLHLVLRDCFTERPSPSERPSIETVRSQLRGM	
G CY - 1 4	248	IYQVKKGGHN---PMRPSLD-TGETVEIN		PALLHLVLRDCWTERPSPSERPSIEQVRGHLNGM	
G CY - 1 3	252	IYFVKRGGRT---PFRPSLD---DVDDIN		PAMHLVLRDCWDEDPKQRPNIDMVNKLKKNM	
G CY - 1	251	VYNVKKGGLF---PIRPEII---TDIHDVN		PALIALVLRDCWAEVPEDRPTAENICSQMKGL	
G CY - 2	250	-----GNIHDVN		PALIALVLRDCWAEVPEDRPTAENICSQMKGL	
G CY - 3	249	IYRVKKGGSF---PIRPDI---TDVPDVN		PTLIALVLRDCWAEAPEDRPTAENICEQLRDL	
G CY - 5	250	LYMVKKGGNR---TIRP-EL---ILDAEVS		PRLTTLVLRDCWSEQPEDRPKAEQICKLLSEM	
G CY - 4	252	KYAVKKGQF---VLRP-DL---HIDIEVNT		LLALVLRDCWCENPEERPSAENVCKVLFDM	
G CY - 9	282	TLAMANDDDQ---LIRPTFPSSNTGEGYN		LQLLSCIEACWLEIPEMRPPIKKVRTMVNAN	
G CY - 1 0	287	LIIKQILNENH---MPRIT---DDYRQEN		NMLLEMCKECWDRNEDKRPPTIKKLIESI	
DAF - 1 1	290	VLIDDENDAIASRFPLPIIIP---EGIEMH		NDLIKMLENCFG---SVRPDIALARKIIDTV	
G CY - 1 2	269	ECRALVEKTVRRVYSDPYFRPDTSDLEVM		QNYVKEVMAACWHHDPEYQRPPEFKTIRNKLKPL	
dGC 1	252	VDYVKKLPLKGEDPFRPEVESIEEAESC		PDYVLACIRDCWAEDEPERPEFSVIRNRLKMK	
rANP - A	270	IERVTRGGEQP---PFRPSMD---L-QSHLE		ELGQLMQRCAWAEDEPERPPFQQIRLALRKF	
eNP - B	272	VQKVRNGQKP---YFRPTTD---T-SCHSE		ELSLIMEGCWAEDEPADRPDPSYIKIFVMKL	
hRetGC - 1	264	VQRVR-SPPP---LCRPLVS---M-DQAP		VECI LLMKQCWAEQPELRPSMDHTFDL	
rGC - D	270	IRKVA-SPPP---LCRPLVS---P-DQGP		LECIQLMQLCWEAEPDRPSLDQIY	

Figure 7.—Continued.

Hsp90 acts as a general chaperone for folding all newly synthesized proteins. For example, an *S. cerevisiae* temperature-sensitive defect in *hsp82* (the Hsp90 ortholog) does not lead to a widespread accumulation of unfolded proteins (Nathan *et al.* 1997).

The rules governing the specificity of Hsp90 interaction with target proteins seem elusive. Hsp90 is promiscuous in that it interacts with targets as varied as nuclear hormone receptors, kinases, tubulin, nitric oxide synthase, and telomerase (see Buchner 1999 for a summary). Yet Hsp90 can also be quite selective, illustrated by the fact that Hsp90 is far more important for v-src kinase function than that of the nearly identical c-src (Xu and Lindquist 1993; Xu *et al.* 1999). Because Hsp90 target proteins do not share common sequences or known structural motifs, it has been hypothesized that Hsp90 recognizes unfolded structures of proteins with complex folding pathways or with unstable intermediates. Complexes of Hsp90 and target proteins also include different assortments of conserved cochaperones and Hsp90 partner proteins (reviewed in Scheibel and Buchner 1998; Buchner 1999; Caplan 1999).

There are homologs of most of these in *C. elegans* (Hsp70 ~ many genes; Hip ~ T12D8.8; Hsp40 ~ F54D5.8; Hop ~ R09E12.3; p23 ~ ZC395.10 (weak homology); Cdc37 ~ W08F4.8; FKBP51 and FKBP52 ~ F31D4.3; Cyp40 ~ none; PP5 ~ Y39B6B.FF; Cns1p ~ C17G10.2). It is intriguing that one of these partner proteins, PP5 (a protein-serine phosphatase) associates with the KHD of the atrial natriuretic peptide receptor (a TM-GC; Chinkers 1994).

On the basis of the known functions of Hsp90, we hypothesize that DAF-21/Hsp90 associates with the DAF-11 TM-GC, perhaps to stabilize an inactive form of the cyclase. This model of physical association can be tested, for example, by coimmunoprecipitation of Hsp90 and DAF-11. An alternative explanation for the shared phenotypes of *daf-11* and *daf-21* mutants is that Hsp90 stabilizes an unidentified protein required for DAF-11-dependent chemosensory transduction. The *daf-21(p673)* E292K mutation causes relatively limited phenotypes (specific sensory defects and reduced fertility) and is not a null mutation. Therefore, the *daf-21(p673)* mutation may interfere relatively specifically

with stabilization of a chemosensory transduction component (such as DAF-11) without seriously impairing other Hsp90 functions. However, a more detailed knowledge of how Hsp90 binds to its targets and cochaperones is needed to understand the consequences of this change.

We thank D. Riddle and P. Albert for the *daf-11(m597)* allele; S. Xu, J. Ahnn, G. Seydoux, and Andy Fire for GFP vectors; Jing Chen and Jill Spoerke (Axys Pharmaceuticals, NemaPharm Group) for generation of the *daf-21(nr2081)* deletion mutation; the *Caenorhabditis* Genetics Center for strains; the *C. elegans* Genome Sequencing Consortium for sequence data and for cosmids; R. Barstead and A. Fire for cDNA libraries; Axys Pharmaceuticals, NemaPharm Group and Cambria Biosciences LLC for resources and equipment; K. Iwasaki for RNA; J. Beavo for advice about 8-bromo-cGMP; S. Yu and D. Garbers for sharing data prior to publication; B. Sawin, C. Trent, H. R. Horvitz, C. Bargmann, M. Ailion, D. Weinschenker, P. Green, D. Pilgrim, K. Kemphues, M. Hengartner, and M. Gilbert for sharing unpublished information. We also thank M. Ailion for helpful comments on the manuscript and C. Bargmann and all members of our laboratory for fruitful conversation. D.A.B. and J.J.V. were supported by National Institutes of Health (NIH) Training Grant T32 GM-07735. E.M.L. was supported by a grant from the American Cancer Society. This work was also supported by NIH grant GM-48700 to J.H.T.

LITERATURE CITED

- Altschul, S. F., W. Gish, W. Miller, E. W. Myers and D. J. Lipman, 1990 Basic local alignment search tool. *J. Mol. Biol.* **215**: 403–410.
- Baehr, W., E. A. Morita, R. J. Swanson and M. L. Applebury, 1982 Characterization of bovine rod outer segment G-protein. *J. Biol. Chem.* **257**: 6452–6460.
- Bargmann, C. I., and H. R. Horvitz, 1991a Control of larval development by chemosensory neurons in *Caenorhabditis elegans*. *Science* **251**: 1243–1246.
- Bargmann, C. I., and H. R. Horvitz, 1991b Chemosensory neurons with overlapping functions direct chemotaxis to multiple chemicals in *C. elegans*. *Neuron* **7**: 729–742.
- Bargmann, C. I., E. Hartwig and H. R. Horvitz, 1993 Odorant-selective genes and neurons mediate olfaction in *C. elegans*. *Cell* **74**: 515–527.
- Barnes, W. M., 1994 PCR amplification of up to 35-kb DNA with high fidelity and high yield from lambda bacteriophage templates. *Proc. Natl. Acad. Sci. USA* **91**: 2216–2220.
- Barstead, R. J., and R. H. Waterston, 1989 The basal component of the nematode dense-body is vinculin. *J. Biol. Chem.* **264**: 10177–10185.
- Bloom, L., and H. R. Horvitz, 1997 The *Caenorhabditis elegans* gene *unc-76* and its human homologs define a new gene family involved in axonal outgrowth and fasciculation. *Proc. Natl. Acad. Sci. USA* **94**: 3414–3419.
- Borkovich, K. A., F. W. Farrelly, D. B. Finkelstein, J. Taulien and S. Lindquist, 1989 hsp82 is an essential protein that is required in higher concentrations for growth of cells at higher temperatures. *Mol. Cell. Biol.* **9**: 3919–3930.
- Brenner, S., 1974 The genetics of *Caenorhabditis elegans*. *Genetics* **77**: 71–94.
- Buchner, J., 1999 Hsp90 & Co.—a holding for folding. *Trends Biochem. Sci.* **24**: 136–141.
- C. elegans* Sequencing Consortium 1998 Genome sequence of the nematode *C. elegans*: a platform for investigating biology. *Science* **282**: 2012–2018.
- Caplan, A. J., 1999 Hsp90's secrets unfold: new insights from structural and functional studies. *Trends Cell Biol.* **9**: 262–268.
- Cassada, R., and R. L. Russell, 1975 The dauer larva, a post-embryonic developmental variant of the nematode *Caenorhabditis elegans*. *Dev. Biol.* **46**: 326–342.
- Chalfie, M., Y. Tu, G. Euskirchen, W. W. Ward and D. C. Prasher, 1994 Green fluorescent protein as a marker for gene expression. *Science* **263**: 802–805.
- Chen, C. F., Y. Chen, K. Dai, P. L. Chen, D. J. Riley *et al.*, 1996 A new member of the hsp90 family of molecular chaperones interacts with the retinoblastoma protein during mitosis and after heat shock. *Mol. Cell. Biol.* **16**: 4691–4699.
- Chinkers, M., 1994 Targeting of a distinctive protein-serine phosphatase to the protein kinase-like domain of the atrial natriuretic peptide receptor. *Proc. Natl. Acad. Sci. USA* **91**: 11075–11079.
- Chinkers, M., and D. L. Garbers, 1989 The protein kinase domain of the ANP receptor is required for signaling. *Science* **245**: 1392–1394.
- Chinkers, M., D. L. Garbers, M. S. Chang, D. G. Lowe, H. M. Chin *et al.*, 1989 A membrane form of guanylate cyclase is an atrial natriuretic peptide receptor. *Nature* **338**: 78–83.
- Chinkers, M., S. Singh and D. L. Garbers, 1991 Adenine nucleotides are required for activation of rat atrial natriuretic peptide receptor/guanylyl cyclase expressed in a baculovirus system. *J. Biol. Chem.* **266**: 4088–4093.
- Coburn, C. M., and C. I. Bargmann, 1996 A putative cyclic nucleotide-gated channel is required for sensory development and function in *C. elegans*. *Neuron* **17**: 695–706.
- Coburn, C. M., I. Mori, Y. Ohshima, C. I. Bargmann, 1998 A cyclic nucleotide-gated channel inhibits sensory axon outgrowth in larval and adult *Caenorhabditis elegans*: a distinct pathway for maintenance of sensory axon structure. *Development* **125**: 249–258.
- Cutforth, T., and G. M. Rubin, 1994 Mutations in Hsp83 and cdc37 impair signaling by the sevenless receptor tyrosine kinase in *Drosophila*. *Cell* **77**: 1027–1036.
- Dalley, B. K., and M. Golomb, 1992 Gene expression in the *Caenorhabditis elegans* dauer larva: developmental regulation of Hsp90 and other genes. *Dev. Biol.* **151**: 80–90.
- Drewett, J. G., and D. L. Garbers, 1994 The family of guanylyl cyclase receptors and their ligands. *Endocr. Rev.* **15**: 135–162.
- Dusenbery, D. B., 1974 Analysis of chemotaxis in the nematode *Caenorhabditis elegans* by countercurrent separation. *J. Exp. Zool.* **188**: 41–48.
- Estevez, M., L. Attisano, J. L. Wrana, P. S. Albert, J. Massague *et al.*, 1993 The *daf-4* gene encodes a bone morphogenetic protein receptor controlling *C. elegans* dauer larva development. *Nature* **365**: 644–649.
- Fesenko, E. E., S. S. Kolesnikov and A. L. Lyubarsky, 1985 Induction by cyclic GMP of cationic conductance in plasma membrane of retinal rod outer segment. *Nature* **313**: 310–313.
- Freeman, B. C., and R. I. Morimoto, 1996 The human cytosolic molecular chaperones hsp90, hsp70 (hsc70) and hdj-1 have distinct roles in recognition of a non-native protein and protein refolding. *EMBO J.* **15**: 2969–2979.
- Frohman, M. A., M. K. Dush and G. R. Martin, 1988 Rapid production of full-length cDNAs from rare transcripts: amplification using a single gene-specific oligonucleotide primer. *Proc. Natl. Acad. Sci. USA* **85**: 8998–9002.
- Georgi, L. L., P. S. Albert and D. L. Riddle, 1990 *daf-1*, a *C. elegans* gene controlling dauer larva development, encodes a novel receptor protein kinase. *Cell* **61**: 635–645.
- Golden, J. W., and D. L. Riddle, 1982 A pheromone influences larval development in the nematode *Caenorhabditis elegans*. *Science* **218**: 578–580.
- Golden, J. W., and D. L. Riddle, 1984a The *Caenorhabditis elegans* dauer larva: developmental effects of pheromone, food, and temperature. *Dev. Biol.* **102**: 368–378.
- Golden, J. W., and D. L. Riddle, 1984b A *Caenorhabditis elegans* dauer-inducing pheromone and an antagonistic component of the food supply. *J. Chem. Ecol.* **10**: 1265–1280.
- Gottlieb, S., and G. Ruvkun, 1994 *daf-2*, *daf-16* and *daf-23*: genetically interacting genes controlling dauer formation in *Caenorhabditis elegans*. *Genetics* **137**: 107–120.
- Goy, M. F., 1991 cGMP: the wayward child of the cyclic nucleotide family. *Trends Neurosci.* **14**: 293–299.
- Grenert, J. P., B. D. Johnson and D. O. Toft, 1999 The importance of ATP binding and hydrolysis by hsp90 in formation and function of protein heterocomplexes. *J. Biol. Chem.* **274**: 17525–17533.
- Hanks, S. K., A. M. Quinn and T. Hunter, 1988 The protein kinase family: conserved features and deduced phylogeny of the catalytic domains. *Science* **241**: 42–52.
- Horvitz, H. R., S. Brenner, J. Hodgkin and R. K. Herman, 1979

- A uniform genetic nomenclature for the nematode *Caenorhabditis elegans*. *Mol. Gen. Genet.* **175**: 129–133.
- Huang, L. S., P. Tzou and P. W. Sternberg, 1994 The *lin-15* locus encodes two negative regulators of *Caenorhabditis elegans* vulval development. *Mol. Biol. Cell* **5**: 395–412.
- Hurley, J. B., 1987 Molecular properties of the cGMP cascade of vertebrate photoreceptors. *Annu. Rev. Physiol.* **49**: 793–812.
- Inoue, T., and J. H. Thomas, 2000 Targets of TGF- β signaling in *C. elegans* dauer formation. *Dev. Biol.* **217**: 192–204.
- Jakob, U., H. Lilie, I. Meyer and J. Buchner, 1995 Transient interaction of Hsp90 with early unfolding intermediates of citrate synthase. Implications for heat shock *in vivo*. *J. Biol. Chem.* **270**: 7288–7294.
- Kimura, Y., S. Matsumoto and I. Yahara, 1994 Temperature-sensitive mutants of hsp82 of the budding yeast *Saccharomyces cerevisiae*. *Mol. Gen. Genet.* **242**: 517–527.
- Komatsu, H., I. Mori, J. S. Rhee, N. Akaike and Y. Ohshima, 1996 Mutations in a cyclic nucleotide-gated channel lead to abnormal thermosensation and chemosensation in *C. elegans*. *Neuron* **17**: 707–718.
- Koutalos, Y., and K. W. Yau, 1993 A rich complexity emerges in phototransduction. *Curr. Opin. Neurobiol.* **3**: 513–519.
- Liu, D. W. C., and J. H. Thomas, 1994 Regulation of a periodic motor program in *C. elegans*. *J. Neurosci.* **14**: 1953–1962.
- Liu, L. X., J. M. Spoerckem, E. L. Mulligan, J. Chen, B. Reardon *et al.*, 1999 High-throughput isolation of *Caenorhabditis elegans* deletion mutants. *Genome Res.* **9**: 859–867.
- Malone, E. A., T. Inoue and J. H. Thomas, 1996 Genetic analysis of the roles of *daf-28* and *age-1* in regulating *Caenorhabditis elegans* dauer formation. *Genetics* **143**: 1193–1205.
- Mayer, M. P., and B. Bukau, 1999 Molecular chaperones: the busy life of Hsp90. *Curr. Biol.* **9**: R322–R325.
- Mazzarella, R., G. Pengue, J. Yoon, J. Jones and D. Schlessinger, 1997 Differential expression of XAP5, a candidate disease gene. *Genomics* **45**: 216–219.
- McNeil, L., M. Chinkers and M. Forte, 1995 Identification, characterization, and developmental regulation of a receptor guanylyl cyclase expressed during early stages of *Drosophila* development. *J. Biol. Chem.* **270**: 7189–7196.
- Mello, C. C., J. M. Kramer, D. Stinchcomb and V. Ambros, 1991 Efficient gene transfer in *C. elegans*: extrachromosomal maintenance and integration of transforming sequences. *EMBO J.* **10**: 3959–3970.
- Meng, X., J. Devin, W. P. Sullivan, D. Toft, E. E. Baulieu *et al.*, 1996 Mutational analysis of Hsp90 alpha dimerization and subcellular localization: dimer disruption does not impede “in vivo” interaction with estrogen receptor. *J. Cell Sci.* **109**: 1677–1687.
- Miki, N., J. M. Baraban, J. J. Keirns, J. J. Boyce and M. W. Bitensky, 1975 Purification and properties of the light-activated cyclic nucleotide phosphodiesterase of rod outer segments. *J. Biol. Chem.* **250**: 6320–6327.
- Miller, L. M., J. D. Plenefisch, L. P. Casson and B. J. Meyer, 1988 *xol-1*: a gene that controls the male modes of sex determination and X chromosome dosage compensation in *C. elegans*. *Cell* **55**: 167–183.
- Morris, J. Z., H. A. Tissenbaum and G. Ruvkun, 1996 A phosphatidylinositol-3-OH kinase family member regulating longevity and diapause in *Caenorhabditis elegans*. *Nature* **382**: 536–539.
- Nathan, D. F., M. H. Vos and S. Lindquist, 1997 In vivo functions of the *Saccharomyces cerevisiae* Hsp90 chaperone. *Proc. Natl. Acad. Sci. USA* **94**: 12949–12956.
- Nemoto, T., and N. Sato, 1998 Oligomeric forms of the 90-kDa heat shock protein. *Biochem. J.* **330**: 989–995.
- Nemoto, T., Y. Ohara-Nemoto, M. Ota, T. Takagi and K. Yokoyama, 1995 Mechanism of dimer formation of the 90-kDa heat-shock protein. *Eur. J. Biochem.* **233**: 1–8.
- Obermann, W. M., H. Sondermann, A. A. Russo, N. P. Pavletich and F. U. Hartl, 1998 In vivo function of Hsp90 is dependent on ATP binding and ATP hydrolysis. *J. Cell Biol.* **143**: 901–910.
- Parkinson, S. J., S. L. Carrithers and S. A. Waldman, 1994 Opposing adenine nucleotide-dependent pathways regulate guanylyl cyclase C in rat intestine. *J. Biol. Chem.* **269**: 22683–22690.
- Picard, D., B. Khurshed, M. J. Garabedian, M. G. Fortin, S. Lindquist *et al.*, 1990 Reduced levels of hsp90 compromise steroid receptor action *in vivo*. *Nature* **348**: 166–168.
- Prodromou, C., S. M. Roem, P. W. Piper and L. H. Pearl, 1997a A molecular clamp in the crystal structure of the N-terminal domain of the yeast Hsp90 chaperone. *Nat. Struct. Biol.* **4**: 477–482.
- Prodromou, C., S. M. Roe, R. O’Brien, J. E. Ladbury, P. W. Piper *et al.*, 1997b Identification and structural characterization of the ATP/ADP-binding site in the Hsp90 molecular chaperone. *Cell* **90**: 65–75.
- Ren, P., C. S. Lim, R. Johnsen, P. S. Albert, D. Pilgrim *et al.*, 1996 Control of *C. elegans* larval development by neuronal expression of a TGF- β homolog. *Science* **274**: 1389–1391.
- Riddle, D. L., and P. S. Albert, 1997 Genetic and environmental regulation of dauer larva development, pp. 739–768 in *C. elegans II*, edited by D. L. Riddle, T. Blumenthal, J. Meyer and J. R. Priess. Cold Spring Harbor Laboratory Press, Plainville, NY.
- Riddle, D. L., M. M. Swanson and P. S. Albert, 1981 Interacting genes in nematode dauer formation. *Nature* **270**: 668–671.
- Schackwitz, W. S., T. Inoue and J. H. Thomas, 1996 Chemosensory neurons function in parallel to mediate a pheromone response in *C. elegans*. *Neuron* **17**: 719–728.
- Scheibel, T., and J. Buchner, 1998 The Hsp90 complex—a super-chaperone machine as a novel drug target. *Biochem. Pharmacol.* **56**: 675–682.
- Scheibel, T., T. Weikl and J. Buchner, 1998 Two chaperone sites in Hsp90 differing in substrate specificity and ATP dependence. *Proc. Natl. Acad. Sci. USA* **95**: 1495–1499.
- Scheibel, T., H. I. Siegmund, R. Jaenicke, P. Ganz, H. Lilie *et al.*, 1999 The charged region of Hsp90 modulates the function of the N-terminal domain. *Proc. Natl. Acad. Sci. USA* **96**: 1297–1302.
- Schumacher, R. J., W. J. Hansen, B. C. Freeman, E. Alnemri, G. Litwack *et al.*, 1996 Cooperative action of Hsp70, Hsp90, and DnaJ proteins in protein renaturation. *Biochemistry* **35**: 14889–14898.
- Singh, S., D. G. Lowe, D. S. Thorpe, H. Rodriguez, W. J. Kuang *et al.*, 1988 Membrane guanylate cyclase is a cell-surface receptor with homology to protein kinases. *Nature* **334**: 708–712.
- Song, H. Y., J. D. Dunbar, Y. X. Zhang, D. Guo and D. B. Donner, 1996 Identification of a protein with homology to hsp90 that binds the type 1 tumor necrosis factor receptor. *J. Biol. Chem.* **271**: 3574–3581.
- Stebbins, C. E., A. A. Russo, C. Schneider, N. Rosen, F. U. Hartl *et al.*, 1997 Crystal structure of an Hsp90-geldanamycin complex: targeting of a protein chaperone by an antitumor agent. *Cell* **89**: 239–250.
- Thomas, J. H., D. A. Birnby and J. J. Vowels, 1993 Evidence for parallel processing of sensory information controlling dauer formation in *Caenorhabditis elegans*. *Genetics* **134**: 1105–1117.
- Troemel, E. R., J. H. Chou, N. D. Dwyer, H. A. Colbert and C. I. Bargmann, 1995 Divergent seven transmembrane receptors are candidate chemosensory receptors in *C. elegans*. *Cell* **83**: 207–218.
- Troemel, E. R., B. E. Kimmel and C. I. Bargmann, 1997 Preprogramming chemotaxis responses: sensory neurons define olfactory preferences in *C. elegans*. *Cell* **91**: 161–169.
- Vaandrager, A. B., E. van der Wiel and H. R. de Jonge, 1993a Heat-stable enterotoxin activation of immunopurified guanylyl cyclase C: modulation by adenine nucleotides. *J. Biol. Chem.* **268**: 19598–19603.
- Vaandrager, A. B., S. Schulz, H. R. De Jonge and D. L. Garbers, 1993b Guanylyl cyclase C is an N-linked glycoprotein receptor that accounts for multiple heat-stable enterotoxin-binding proteins in the intestine. *J. Biol. Chem.* **268**: 2174–2179.
- van der Keyl, H., H. Kim, R. Espey, C. V. Oke and M. K. Edwards, 1994 *Caenorhabditis elegans sqt-3* mutants have mutations in the *col-1* collagen gene. *Dev. Dyn.* **201**: 86–94.
- van der Straten, A., C. Rommel, B. Dickson and E. Hafen, 1997 The heat shock protein 83 (Hsp83) is required for Raf-mediated signalling in *Drosophila*. *EMBO J.* **16**: 1961–1969.
- Vowels, J. J., 1994 Genes mediating chemosensory responses in *Caenorhabditis elegans*. Ph.D. Thesis, University of Washington, Seattle.
- Vowels, J. J., and J. H. Thomas, 1992 Genetic analysis of chemosensory control of dauer formation in *Caenorhabditis elegans*. *Genetics* **130**: 105–123.
- Vowels, J. J., and J. H. Thomas, 1994 Multiple chemosensory defects in *daf-11* and *daf-21* mutants of *Caenorhabditis elegans*. *Genetics* **138**: 303–316.

- Ward, S., 1973 Chemotaxis by the nematode *Caenorhabditis elegans*: identification of attractants and analysis of the response by use of mutants. *Proc. Natl. Acad. Sci. USA* **70**: 817-821.
- Waterston, R., C. Martin, M. Craxton, C. Huynh, A. Coulson *et al.*, 1992 A survey of expressed genes in *C. elegans*. *Nat. Genet.* **1**: 114-123.
- Waterston, R. H., J. E. Sulston and A. R. Coulson, 1997 The genome, pp. 23-45 in *C. elegans II*, edited by D. L. Riddle, T. Blumenthal, B. J. Meyer and J. R. Priess. Cold Spring Harbor Laboratory Press, Cold Spring Harbor, NY.
- Weich, H., J. Buchner, R. Zimmerman and U. Jakob, 1992 Hsp90 chaperones protein folding *in vitro*. *Nature* **358**: 169-170.
- Welch, W. J., and J. R. Feramisco, 1982 Purification of the major mammalian heat shock proteins. *J. Biol. Chem.* **257**: 14949-14959.
- White, J. G., E. Southgate, J. N. Thomson and S. Brenner, 1986 The structure of the nervous system of the nematode *Caenorhabditis elegans*. *Philos. Trans. R. Soc. Lond. B* **314**: 1-340.
- Wood, W. B. (Editor), 1988 *The Nematode Caenorhabditis elegans*. Cold Spring Harbor Laboratory Press, Cold Spring Harbor, NY.
- Xu, Y., and S. Lindquist, 1993 Heat-shock protein hsp90 governs the activity of pp60v-src kinase. *Proc. Natl. Acad. Sci. USA* **90**: 7074-7078.
- Xu, Y., M. A. Singer and S. Lindquist, 1999 Maturation of the tyrosine kinase c-src as a kinase and as a substrate depends on the molecular chaperone Hsp90. *Proc. Natl. Acad. Sci. USA* **96**: 109-114.
- Young, J. C., C. Schneider and F. U. Hartl, 1997 In vitro evidence that hsp90 contains two independent chaperone sites. *FEBS Lett.* **418**: 139-143.
- Yu, S., L. Avery, E. Baude and D. L. Garbers, 1997 Guanylyl cyclase expression in specific sensory neurons: a new family of chemosensory receptors. *Proc. Natl. Acad. Sci. USA* **94**: 3384-3387.
- Yuen, P. S. T., and D. L. Garbers, 1992 Guanylyl cyclase-linked receptors. *Annu. Rev. Neurosci.* **15**: 193-225.
- Zwaal, R. R., A. Broeks, J. van Meurs, J. T. Groenen and R. H. Plasterk, 1993 Target-selected gene inactivation in *Caenorhabditis elegans* by using a frozen transposon insertion mutant bank. *Proc. Natl. Acad. Sci. USA* **90**: 7431-7435.
- Zwaal, R. R., J. E. Mendel, P. W. Sternberg and R. H. A. Plasterk, 1997 Two neuronal G proteins are involved in chemosensation of the *C. elegans* dauer inducing pheromone. *Genetics* **145**: 715-727.

Communicating editor: I. Greenwald